Radboud Universiteit

Master Thesis

Free the Penguin!

Studying $B^- \to K^- \nu\bar{\nu}$ Backgrounds

Nora Locht
Author

Dr. Danny van Dyk
Supervisor

Dr. Susanne Westhoff
Supervisor

The Standard Model of particle physics is a very powerful model but has its limits. We studied the process $B^- \to K^- \nu\bar{\nu}$, where the difference between the predicted branching ratio $\mathcal{B}_{\text{Theory}}(B^- \to K^- \nu\bar{\nu}) = (5.58 \pm 0.37) \times 10^{-6}$ and the measured branching ratio $\mathcal{B}_{\text{Exp}}(B^- \to K^- \nu\bar{\nu}) = (2.3 \pm 0.7) \times 10^{-5}$ leaves room for physics beyond the Standard Model. To study two lepton-mediated backgrounds to the signal process, we use the weak effective theory. We show that the kinematic dependence of the differential branching ratio could be different in the case of new physics. Therefore a part of the analysis of the experimental data on this background needs to be redone in order to take new physics into account.

Contents

Chapter 1

Introduction

You and I and everything around us is made up of atoms. Atoms consist of a nucleus surrounded by one or more electrons. These electrons seem to be indivisible: they are fundamental building blocks of the universe. The nucleus, however, is built of protons and neutrons, which themselves are built of quarks and some glue to hold them together. In turn, these quarks form fundamental building blocks, and so do the particles – gluons – that make up the glue. The Standard Model is the theory that describes how these and other fundamental particles in the universe interact. Many predictions of the Standard Model have been tested thoroughly in several colliders throughout the years.
The Standard Model is one of the most successful theories in physics. It was able to predict several properties, including particles such as the Higgs boson, that were later experimentally observed. However, there are some things that the Standard Model cannot explain yet. For example, the Standard Model does not describe gravity. Also, the Standard Model does not predict unequal amounts of matter and antimatter in the universe, but much more matter than antimatter is observed. In addition, as we look at the rotation of stars and galaxies in the universe, some mass appears to be missing. There must be some particles that have mass that we are not yet able to detect. Therefore it is important to test the Standard Model even further and search for new physics beyond the Standard Model.

In search of physics beyond the Standard Model, this thesis focuses on the process $B^- \to K^- \nu\bar{\nu}$. B is a bottom meson: a quark-antiquark pair of which the heaviest constituent is a bottom quark. K is a kaon: a quark-antiquark pair of which the heaviest quark is a strange quark. ν and $\bar{\nu}$ are, respectively, a neutrino and an antineutrino.
$B^- \to K^- \nu\bar{\nu}$ is a rare decay: the Standard Model branching ratio of the $(B^- \to K^- \nu\bar{\nu})$ decay is predicted in [1] to be $\mathcal{B}_{\text{Theory}}(B^- \to K^- \nu\bar{\nu}) = (5.58 \pm 0.37) \times 10^{-6}$. Recently, the main contribution to $B^- \to K^- \nu\bar{\nu}$ is measured at Belle II to have a branching ratio of $\mathcal{B}_{\text{Exp}}(B^- \to K^- \nu\bar{\nu}) = (2.3 \pm 0.7) \times 10^{-5}$ [2]. This experimental result is 2.7 standard deviations above the Standard Model expectation. It opens the door for new physics: imagine a new, rare interaction mediating, among others, $B^- \to K^- \nu\bar{\nu}$. It would be easier to measure this interaction in a process where it contributes significantly compared to a small Standard Model contribution and could therefore increase the measurement. This possibility is researched in several papers, including [3] and [4].
Another possible explanation for this difference lies in the fact that the two final state neutrinos are not reconstructed directly. Therefore the B^- meson could decay into a kaon and an undetectable

particle, mimicking the neutrinos. Candidates for such particles include an axionlike particle [5] [6] or a dark-sector mediator [7], among others [8].

The prominent diagram for $B^- \to K^-\nu\bar{\nu}$ can be seen in Figure 1.1. This diagram is called a penguin diagram. In this case, the $B^- \to K^-\nu\bar{\nu}$ loop-induced process is mediated by an up-type quark and a W boson. For the rest of this thesis, this process is called the signal.

However, $B^- \to K^-\nu\bar{\nu}$ can also take place via leptonic decay, as can be seen in Figure 1.2.

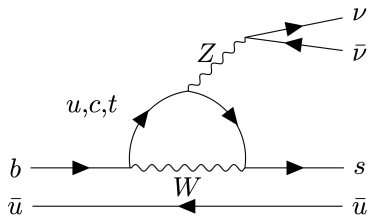

Figure 1.1 The signal: the meson changes flavor twice, with the help of a W boson. The up-type quark that mediates this process emits a Z boson, which decays into a $\nu\bar{\nu}$ pair.

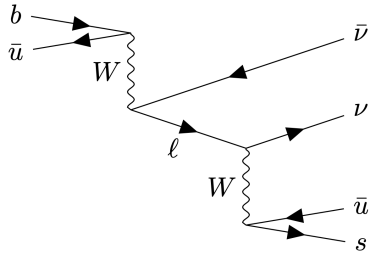

Figure 1.2 Background process I: the $B^- \to \ell^-[\to K^-\nu]\bar{\nu}$ process via leptonic decay. The B meson decays into a lepton with arbitrary flavor, ℓ^-, and the corresponding neutrino $\bar{\nu_\ell}$. The lepton then decays further into a Kaon and a ν_ℓ.

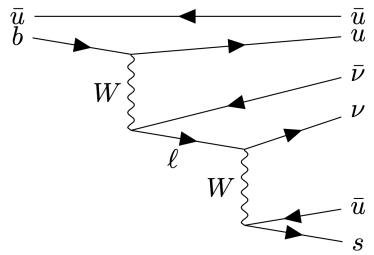

Figure 1.3 Background process 2: the $B^- \to \pi^0\ell^-[\to K^-\nu]\bar{\nu}$ process via leptonic decay. The B meson decays into a neutral pion, an arbitrary lepton, $\bar{\ell}$, and the corresponding neutrino ν_ℓ. The lepton then decays further into a Kaon and a $\bar{\nu_\ell}$.

The process, $B^- \to \tau[\to K^-\nu]\bar{\nu}$, which has a τ as an intermediate state, is the most important background to the signal. The general process $B^- \to \ell[\to K^-\nu]\bar{\nu}$ will be called background process I. We can see that the signal and background process I $B^- \to \ell[\to K^-\nu]\bar{\nu}$ have the same particle composition in the end, and the only way to distinguish the two processes is through the kinematic distribution of the Kaon. Since the processes cannot be distinguished from each other by particle content, even in a perfect detector, the background is an irreducible background.

We now look at another diagram, $B^- \to \pi^0 \ell[\to K^- \nu]\bar{\nu}$, as can be seen in Figure 1.3. Since the π^0 is long-lived and carries no electromagnetic charge, it can easily be missed in a detector. Therefore, it too is a background to the signal. In an ideal world, with ideal detectors, one could detect these particles, and the two processes would be distinguishable from one another. Therefore, this process is called a reducible background. This process is similar to background process I except that there is a pion in the final state. Due to the similarities in the backgrounds, we choose to study this background additionally. It will be called background process II.

In [9], the decay width of both the signal and the background is calculated using the Standard Model. Since we are looking for physics beyond the Standard Model, it is interesting to determine the decay width in a way which includes all possible contributions beyond the Standard Model, which are due to particles much heavier than the B^- meson. In [10] the signal is analyzed in the Standard Model as well as in several new physics models. In this thesis, the backgrounds are studied in the Standard Model and beyond, using a Weak Effective Theory.

Chapter 2

The Standard Model

In the Standard Model (SM), the signal as well as the background are described by electroweak interactions. For this reason, this chapter will mainly focus on the electroweak properties of the SM, and will not describe the rest of the SM, e.g., the strong force or the Higgs mechanism.
This chapter describes the electromagnetic and the weak force before describing how the hypercharge force and the weak force are united in the SM. It dives a little deeper into flavor physics before it describes some properties within the SM needed for our calculations.

2.1 The Electromagnetic Force

The SM is constructed with bosons and leptons. It contains several bosons: the electroweak bosons $W^{\pm}$ and Z, photons γ, the gluons g and H, and the Higgs boson. They couple with each other and with a total of twelve fermions and their antifermions. For the electromagnetic force, the only relevant boson is the photon γ.
The photon γ is the boson of the electromagnetic sector. It couples to all charged particles. This includes all quarks, the charged leptons and the $W^{\pm}$ boson.
There is only one interaction possible for the electromagnetic sector, shown in Figure 2.1. The particle the photon γ couples with stays unchanged in this interaction.

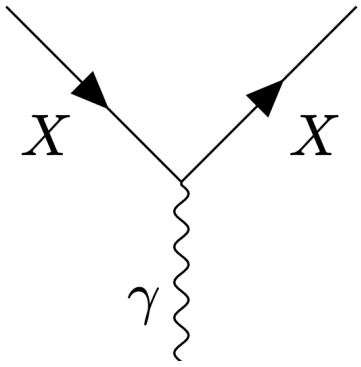

Figure 2.1 The interaction of a γ particle. X represents any charged particle.

2.2 The Weak Forces

The weak sector has three bosons: the charged bosons $W^{\pm}$ and the neutral boson Z. The Z boson couples as the photon does, but with different coupling strength to different fermions and additionally it couples to the neutrinos ν. As in the case of the photon, the Z cannot change the type of particle it is interacting with.
Two important concepts to introduce in the context of the weak interaction are helicity and chirality. The projection of the spin of a particle onto its momentum direction is called helicity. A particle is called right-handed if the helicity of the particle is positive. If the helicity of the particle is negative, the particle is called left-handed. Chirality is an intrinsic, Lorentz invariant property of a particle. It denotes the particle's preferred helicity. In the case of massless particles, these two coincide. However, in the case of massive particles, the frame of reference may change the helicity of a particle. The weak force only couples to particles with left-handed chirality.

The left- and right-handed fields can be found using the projection operators on a Dirac spinor ψ

$$\psi_L = P_L\psi \qquad\qquad \psi_R = P_R\psi, \tag{2.1}$$

where the projection operators are defined as

$$P_L = \frac{1-\gamma_5}{2} \qquad\qquad P_R = \frac{1+\gamma_5}{2}. \tag{2.2}$$

The $W^{\pm}$ particles are charged particles, one positively charged, the other negatively charged. The $W^{\pm}$ bosons couple to all fermions and all electroweak bosons. In all interactions in the SM, electromagnetic charge is conserved. Since the $W^{\pm}$ bosons are charged, the interactions pictured above mediated by the Z and γ bosons are only possible for the $W^{\pm}$ bosons if they are the particle named X. Additionally, the interactions of the $W^{\pm}$ boson with the leptons change the particle the $W^{\pm}$ boson interacts with into the lepton's SU(2) doublet partner:

$$L_L = \begin{pmatrix} \nu_\ell \\ \ell \end{pmatrix}_L \qquad\qquad Q_L = \begin{pmatrix} u \\ d \end{pmatrix}_L, \tag{2.3}$$

where u can be any up-type quark, d can be any down-type quark, and ℓ any type of lepton. The subscript L denotes the left-handedness of the particles.
The interactions of the Z and $W^{\pm}$ bosons stated above are shown in Figure 2.2.

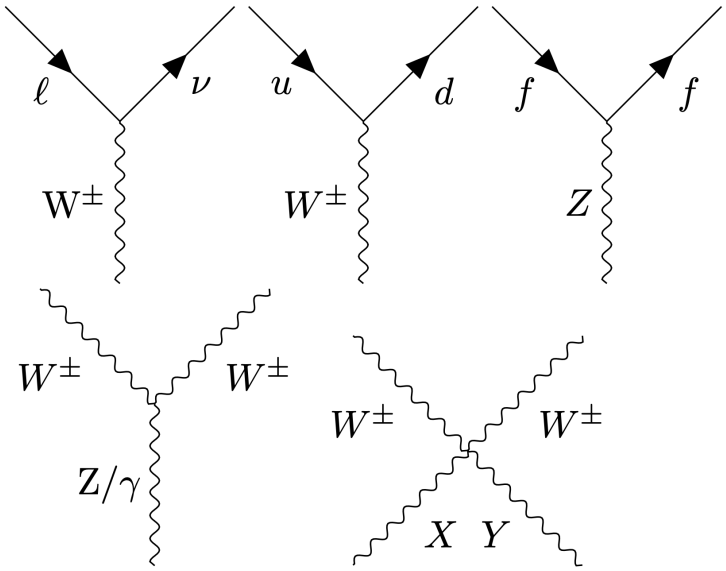

Figure 2.2 The interactions of the Z and $W^{\pm}$ bosons: $W^{\pm}$ coupling to the lepton doublet and the quark doublet, Z coupling to any fermions, and the couplings of the bosons onto other bosons. X and Y can be any combination of bosons such that electromagnetic charge is conserved in the interaction.

2.3 Electroweak sector

The electroweak sector in the SM combines and describes the combination of the electromagnetic sector and the weak sector into one $SU(2)_L \times U(1)_Y$ gauge group. The bosons in this group are W^1, W^2, W^3 and B.

Due to the Higgs mechanism, electroweak symmetry breaking occurs spontaneously. This symmetry breaking has several important consequences. Firstly, the four bosons of the $SU(2)_L \times U(1)_Y$ gauge group recombine to form the bosons in the electromagnetic and the weak force in the following way:

$$W^{\pm} = \frac{W^1 \mp iW^2}{\sqrt{2}} \tag{2.4}$$

$$Z = \cos\theta_W W^3 - \sin\theta_W B \tag{2.5}$$

$$\gamma = \sin\theta_W W^3 + \cos\theta_W B\,, \tag{2.6}$$

where θ_W is the weak mixing angle. These combinations give back the known $U(1)_{EW}$ gauge group again.

After electroweak symmetry breaking, the $W^{\pm}$ and the Z bosons have mass, whereas the γ boson remains massless. The $W^{\pm}$ boson has a mass of 80.377 ± 0.012 GeV. The Z boson has a mass of 91.1876 ± 0.0021 GeV.[11]

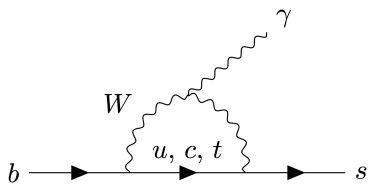

Figure 2.3 An example of an FCNC interaction, in this case a b going to an s, emitting a γ. The process is mediated by a $W^{\pm}$ boson. The u, c, t can be any flavor up-type quark.

2.4 Flavor Physics

In the SM, the quarks come in three different flavors. The up-type quarks are u, c, and t and are usually called up, charm, and top respectively. The down-type quarks are d, s, and b and are usually called down, strange, and bottom respectively. The $W^{\pm}$ boson couples with the $SU(2)_L$ doublets stated in equation 2.3. So, in principle, the $W^{\pm}$ couples the u only to the d. However, the interaction eigenstates with which the $W^{\pm}$ boson couples are not the same as the mass eigenstates. Therefore, there are interactions possible in which a $W^{\pm}$ boson changes any up-type quark to any down-type quark. The coupling strengths of the $W^{\pm}$ interactions are represented in the CKM matrix. Their numerical values [11] are measured to be

$$|V_{CKM}| = \begin{pmatrix} |V_{ud}| & |V_{us}| & |V_{ub}| \\ |V_{cd}| & |V_{cs}| & |V_{cb}| \\ |V_{td}| & |V_{ts}| & |V_{tb}| \end{pmatrix} \tag{2.7}$$

$$= \begin{pmatrix} 0.97435 \pm 0.00016 & 0.22500 \pm 0.00067 & 0.00369 \pm 0.00011 \\ 0.22486 \pm 0.00067 & 0.97349 \pm 0.00016 & 0.04182^{+0.00085}_{-0.00074} \\ 0.00857^{+0.00020}_{-0.00018} & 0.04110^{+0.00083}_{-0.00072} & 0.999118^{+0.000031}_{-0.000036} \end{pmatrix}. \tag{2.8}$$

Processes like these, that change the flavor and the charge of the quark, are called flavor-changing charged-current (FCCC) interactions. Processes that change the flavor of a quark without changing the charge are called flavor-changing neutral-current (FCNC) interactions. Unlike the FCCC interactions, FCNC interactions cannot happen at tree level in the SM since the Z boson does not change flavor. In the SM, FCNC interactions take place in loop diagrams involving a $W^{\pm}$ boson. An example of such a process can be seen in Figure 2.3.

2.5 The GIM Mechanism

The dominant contribution to $B \to K\nu\bar{\nu}$ is the signal process, as displayed in Figure 1.1. Due to the absence of tree-level FCNC interactions, there is a loop in this process. This loop can contain all different up-type quarks. The GIM mechanism as proposed in [12] states that in loop decays the amplitude is proportional to $\frac{m_i^2}{M_W^2}$ [13], where m_i is the mass of the quark in the loop. Therefore the

total amplitude calculated from this diagram is proportional to

$$\mathcal{M} \propto \sum_{i=u,c,t} \frac{m_i^2}{M_W^2} V_{ib} V_{is}^* . \tag{2.9}$$

The CKM matrix is a unitary matrix. From this follows that

$$\sum_{i=u,c,t} V_{ib} V_{is}^* = 0 .$$

Several things arise from this that are important for this thesis. Firstly, the m_i-independent term of this loop amplitude would diverge, but the unitarity of the CKM matrix guarantees that this term is zero. Secondly, there is a suppression of order $\frac{m_i^2}{M_W^2}$ to the amplitude. The rate of this process is tiny and the decay is very hard to observe, due to the loop-suppression.
Lastly the amplitude scales with m_i^2 of the internal quark. Due to this, the decay rate is more sensitive to the heavier quarks. This ensures that the up-type quark in the loop-induced signal process is usually a top quark.

2.6 Decay Constants

Due to the strong force, quarks can never be found alone. Bound states of two quarks, such as the B and K mesons in our process, can therefore not be viewed as two quarks alone. Decay constants summarize how a meson decays and is formed. These decay constants can be found either by comparing decays from measurement or with lattice computations [10].
For the remainder of this thesis, several decay constants are used. For the first background process, the decay constants of the B meson and the kaon are used [14]

$$\langle 0 | \, \bar{u} \gamma_\mu \gamma^5 b \, | B^-(p) \rangle = i f_B p_\mu , \tag{2.10}$$

$$\langle 0 | \, \bar{u} \gamma_\mu \gamma^5 s \, | K^-(k) \rangle = i f_K k_\mu , \tag{2.11}$$

where p_μ and k_μ are the momenta of the B^- meson and the kaon respectively.
For the second background process, including a pion, decay constants for a B meson decaying into a pion and a W^- are used additionally. These decay constants are derived from the form in [15] to be

$$\langle \pi^0(p') | \, \bar{u} \gamma_\mu b \, | B^-(p) \rangle = f_+(P^2) \left[(p+p')_\mu - \frac{M_B^2 - M_\pi^2}{P^2} P_\mu \right] + f_0(P^2) \frac{M_B^2 - M_\pi^2}{P^2} P_\mu , \tag{2.12}$$

$$\langle \pi^0(p') | \, \bar{u} b \, | B_-(p) \rangle = f_0(P^2) \frac{M_B^2 - M_\pi^2}{m_b - m_u} , \tag{2.13}$$

$$\langle \pi^0(p') | \, \bar{u} \sigma_{\mu\nu} b \, | B_-(p) \rangle = i f_T \left[\frac{(p+p')_\mu P_\nu}{M_B + M_\pi} - \frac{M_B - M_\pi}{P^2} P_\mu P_\nu \right] . \tag{2.14}$$

M_B and M_π are the masses of the B meson and the pion, respectively, and P_μ and p'_μ are the momenta of the W^- boson and the pion respectively.

Chapter 3

Weak Effective Theory

No speed can ever exceed the speed of light. To ensure physics never predicts speeds beyond this speed, the Newtonian laws of motion are adjusted. This new, complete theory of motion called special relativity describes physics for all speeds. However, in talking about speeds that we observe in our daily life – how fast a person runs, for example – the fact that nothing can ever exceed the speed of light plays no role at all. Since both sets of rules give us the same outcome, we use the simpler, Newtonian laws of motion that do not take relativistic effects into account. These simpler, Newtonian laws are then an effective theory.

There are several areas in physics where effective field theories come in handy. For example, the energies in a Hydrogen atom are computed using an effective theory [14]. Historically, the Fermi theory of weak interactions has been used to describe weak interactions at energies below the W and Z masses. Whereas our first example was a low-speed effective theory, this is a low-energy effective field theory (EFT). EFTs are full-fledged quantum theories with which one can compute measurable quantities without any reference or input from an underlying high-energy theory.

This thesis makes use of a low-energy effective field theory. For the processes discussed in this thesis, the energy scale at which the processes take place is approximately M_B, the mass of the B meson. Everything that is only relevant at energies $E \gg M_B$ is irrelevant and therefore omitted from our theory.

The mass of the B^- meson M_B is much smaller than the mass of the $W^\pm$ and the Z bosons. To compare: [11]

$$M_B = 5.27934 \pm 0.00012\text{GeV}, \tag{3.1}$$

$$M_W = 80.377 \pm 0.012\text{GeV} \tag{3.2}$$

$$M_Z = 91.1876 \pm 0.0021\text{GeV}. \tag{3.3}$$

From this follows that the $W^\pm$ boson in our $B^- \to K^- \nu\bar{\nu}$ process can never be on shell. We can thus make use of an effective theory from which the $W^\pm$ boson is integrated out.

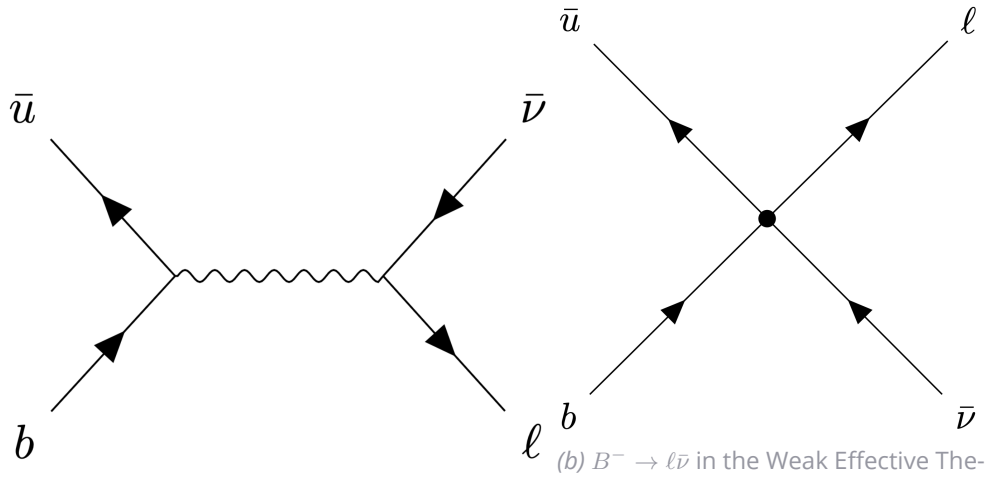

(a) $B^- \to \ell\bar{\nu}$ in the SM

(b) $B^- \to \ell\bar{\nu}$ in the Weak Effective Theory.

Figure 3.1 $B \to \ell\bar{\nu}$ as obtained by integrating out the $W^\pm$ boson in the Standard Model. The crossed circle in Subfigure 3.1b represents a local four-lepton operator in the effective theory.

3.1 Build the Weak Effective Theory

We will build the Weak Effective Theory (WET) from the bottom up. This means that we build a basis of operators without making any connection to a UV complete theory[16] [17]. The basic starting point for phenomenology of weak decays of hadrons is the effective weak Lagrangian which has the generic structure

$$\mathcal{L}_{\mathcal{EFT}} = \frac{4G_F}{\sqrt{2}} V_{jk} \sum_i \mathcal{C}_i \mathcal{O}_i \,, \tag{3.4}$$

in which G_F is the Fermi constant, V_{jk} is the relevant component of V_{CKM} from equation 2.7, dimensionful $\mathcal{O}_i$ are the relevant local operators which govern the decays in question, and C_i the dimensionless Wilson Coefficients that describe the interaction strength of the given operator. Note that the Wilson coefficients C_i are process independent, i.e., the same coefficients arise in the calculation of many different weak-interaction amplitudes. The operators $\mathcal{O}_i$ consist of the light fields only. The locality of the operators ensures that a separation of energy scales can be realized in the WET.

For an example of this, see $B \to \ell\bar{\nu}$, the first part of the first background process considered in this thesis. In the SM case there is only one operator contributing, and the effective Lagrangian takes the form

$$\mathcal{L}^{ub\ell\nu} = \frac{4G_F}{\sqrt{2}} V_{ub} \mathcal{C}_{V_{L,L}} [\bar{\ell}\gamma^\mu P_L \nu] \, [\bar{u}\gamma_\mu P_L b] + h.c. \,. \tag{3.5}$$

In this case the Wilson coefficient is $\mathcal{C}_{V_{L,L}} = 1$, the first brackets show the leptonic current, in this case producing a lepton and its neutrino, and the second brackets show the hadronic current. This operator is represented by the diagram in Figure 3.1.

3.2 Extending the Theory Beyond the SM

Since the $W^{\pm}$ boson is integrated out now, the SM can be extended with beyond-the-SM operators. The operators represent the low-energy interactions corresponding to hypothetical particles like the $W^{\pm}$ boson that mediate these processes.
From the operators mediating $B^- \to \ell^- \bar{\nu}$, the dominant contributions in the short-distance expansion come from the operators with lowest mass dimension. In our case these are four-fermion operators of mass dimension six. Consider all linearly independent operators that respect the SM symmetries: Lorentz and SM gauge symmetry. For the example mentioned above, $B \to \ell\bar{\nu}$, the operators with mass dimension six are

$$\begin{aligned}
\mathcal{O}_{V,L,L} &= \left[\bar{u}\gamma^\mu P_L b\right]\left[\bar{\ell}\gamma_\mu P_L \nu\right], & \mathcal{O}_{V,R,L} &= \left[\bar{u}\gamma^\mu P_R b\right]\left[\bar{\ell}\gamma_\mu P_L \nu\right], \\
\mathcal{O}_{S,L,L} &= \left[\bar{u} P_L b\right]\left[\bar{\ell} P_L \nu\right], & \mathcal{O}_{S,R,L} &= \left[\bar{u} P_R b\right]\left[\bar{\ell} P_L \nu\right], \\
\mathcal{O}_{T,L} &= \left[\bar{u}\sigma^{\mu\nu} b\right]\left[\bar{\ell}\sigma_{\mu\nu} P_L \nu\right], & & \\
\mathcal{O}_{V,L,R} &= \left[\bar{u}\gamma^\mu P_L b\right]\left[\bar{\ell}\gamma_\mu P_R \nu\right], & \mathcal{O}_{V,R,R} &= \left[\bar{u}\gamma^\mu P_R b\right]\left[\bar{\ell}\gamma_\mu P_R \nu\right], \\
\mathcal{O}_{S,L,R} &= \left[\bar{u} P_L b\right]\left[\bar{\ell} P_R \nu\right], & \mathcal{O}_{S,R,R} &= \left[\bar{u} P_R b\right]\left[\bar{\ell} P_R \nu\right], \\
\mathcal{O}_{T,R} &= \left[\bar{u}\sigma^{\mu\nu} b\right]\left[\bar{\ell}\sigma_{\mu\nu} P_R \nu\right].
\end{aligned} \tag{3.6}$$

In these operators, we define $\sigma^{\mu\nu} = \frac{i}{2}[\gamma^\mu, \gamma^\nu]$, in terms of the Dirac matrices, using the same convention as [18]. The operators are labeled as follows: The subscript V denotes a left-handed vector current, the subscript S a scalar current and the subscript T a tensor current, the first L or R refers to the chirality of the quarks, whereas the second L or R refers to the chirality of the leptons. Beyond these operators, the operators with mass dimension seven contribute most. However, effects of these operators, and operators with mass dimension of 8 or higher, are suppressed by at least an extra factor of $\frac{M_B}{M_W}$ and can therefore be neglected in weak decays of mesons.
The Lagrangian for the process $B \to \ell\bar{\nu}$ is thus the Lagrangian expressed in equation 3.4 with operators expressed in equation 3.6. For clarity, the SM Lagrangian is reconstructed from the full Lagrangian by setting all Wilson coefficients C_i to zero, except $\mathcal{O}_{V,L,L} = 1$.
The above operators are constructed for the decay $B \to \ell\bar{\nu}$, but Lagrangians for other processes to be described by WET in this thesis follow the same structure.

Chapter 4

Background Process I: $B^- \to \ell^- \left[\to K^- \nu\right] \bar{\nu}$

The aim of this chapter is to analyze the lepton-mediated cascade $B^- \to \ell^- [\to K^- \nu] \bar{\nu}$, in the SM and beyond. The Feynman diagram of this process can be viewed in Figure 4.1. To do this, we define the momenta of the process as

$$B^-(p) \to \ell^-(Q) \left[\to K^-(k)\nu(q_1)\right] \bar{\nu}(q_2)\,. \tag{4.1}$$

Additionally, we define $q^2 = (q_1 + q_2)^2$, the four-momentum of the neutrinos added and then squared. This is the momentum that is missed in the detector. The expression for this can be found in Appendix A.
The final analytical answer will be a differential branching ratio of the form $\frac{d\mathcal{B}}{dq^2}(q^2)$, to enable comparison of our theory predictions with experimental data as much as possible. Since the neutrinos are not detected directly, there is only one independent kinematic observable in which to express our branching ratio. In experimental research, such as [2], the kinematic dependence on q^2 is used to distinguish between the signal and the background. Literature studying the signal process, such as [10], [8], as well as literature studying the background process [9], use this or a similar format. Therefore, we choose to express our differential branching ratio in the same manner. To get to the differential branching ratio, we will start with the Lagrangian of interactions contributing to this process, shaping the operators and the decay constants used into the right form. The differential branching ratio of this process is found using

$$d\mathcal{B} = \frac{(2\pi)^4}{2M_B\Gamma_B} \left\langle |\mathcal{M}|^2 \right\rangle d\Phi_3(p; k, q_1, q_2)\,, \tag{4.2}$$

therefore subsequently the amplitude $\mathcal{M}$, its spin-averaged square $\left\langle |\mathcal{M}|^2 \right\rangle$ and the three-body phase space element $d\Phi_3(p; k, q_1, q_2)$ are computed. Once the branching ratio is computed, it is plotted and analyzed. The chapter is concluded with a brief section on the interference between the signal and this background process.

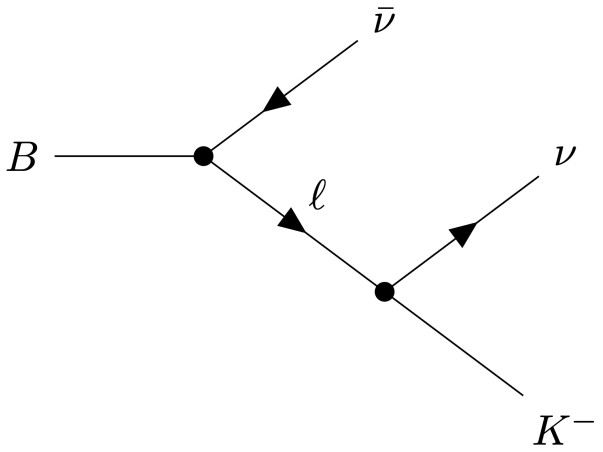

Figure 4.1 A diagram of the first background process $B^- \to \ell^- [\to K^- \nu] \bar{\nu}$, in the Weak Effective Theory.

4.1 The Operators

Since this decay is a cascade, the two parts of the process are described separately first and then used as the first ingredients for the differential decay width. In section 4.3 it becomes clear why this is possible.
For the description of the first part of the process, $B^- \to \ell^- \bar{\nu}$, the following effective Lagrangian is used, as introduced in chapter 3:

$$\mathcal{L}^{ub\ell\nu} = \frac{4G_F}{\sqrt{2}} V_{ub} \sum_i \mathcal{C}_i^{ub\ell\nu} \mathcal{O}_i^{ub\ell\nu} \,. \tag{4.3}$$

We divide the operators into two sets, being

$$\begin{aligned} \mathcal{O}_{V,L,L}^{ub\ell\nu} &= \left[\bar{u}\gamma^\mu P_L b\right] \left[\bar{\ell}\gamma_\mu P_L \nu\right], & \mathcal{O}_{V,R,L}^{ub\ell\nu} &= \left[\bar{u}\gamma^\mu P_R b\right] \left[\bar{\ell}\gamma_\mu P_L \nu\right], \\ \mathcal{O}_{S,L,L}^{ub\ell\nu} &= \left[\bar{u} P_L b\right] \left[\bar{\ell} P_L \nu\right], & \mathcal{O}_{S,R,L}^{ub\ell\nu} &= \left[\bar{u} P_R b\right] \left[\bar{\ell} P_L \nu\right], \\ \mathcal{O}_{T,L}^{ub\ell\nu} &= \left[\bar{u}\sigma^{\mu\nu} b\right] \left[\bar{\ell}\sigma_{\mu\nu} P_L \nu\right], \end{aligned} \tag{4.4}$$

with only left-handed neutrinos, and

$$\begin{aligned} \mathcal{O}_{V,L,R}^{ub\ell\nu} &= \left[\bar{u}\gamma^\mu P_L b\right] \left[\bar{\ell}\gamma_\mu P_R \nu\right], & \mathcal{O}_{V,R,R}^{ub\ell\nu} &= \left[\bar{u}\gamma^\mu P_R b\right] \left[\bar{\ell}\gamma_\mu P_R \nu\right], \\ \mathcal{O}_{S,L,R}^{ub\ell\nu} &= \left[\bar{u} P_L b\right] \left[\bar{\ell} P_R \nu\right], & \mathcal{O}_{S,R,R}^{ub\ell\nu} &= \left[\bar{u} P_R b\right] \left[\bar{\ell} P_R \nu\right], \\ \mathcal{O}_{T,R}^{ub\ell\nu} &= \left[\bar{u}\sigma^{\mu\nu} b\right] \left[\bar{\ell}\sigma_{\mu\nu} P_R \nu\right], \end{aligned} \tag{4.5}$$

where right-handed neutrinos are added to the theory.
For the second half of the process, $\ell^- \to K^- \nu$, the following effective Lagrangian is used:

$$\mathcal{L}^{\ell\nu us} = \frac{4G_F}{\sqrt{2}} V_{us} \sum_i \mathcal{C}_i^{us\ell\nu,*} \mathcal{O}_i^{us\ell\nu,\dagger} \,. \tag{4.6}$$

The operators $\mathcal{O}_i^{us\ell\nu}$ are constructed in the same way as in equation 4.4 and equation 4.5, after which their complex conjugate is computed. The operators $\mathcal{O}_i^{us\ell\nu}$ for $K^- \to \ell^-\bar{\nu}$ in equivalence to equation 4.4 are

$$\begin{aligned}
\mathcal{O}_{V,L,L}^{us\ell\nu} &= \left[\bar{u}\gamma^\mu P_L s\right]\left[\bar{\ell}\gamma_\mu P_L \nu\right], & \mathcal{O}_{V,R,L}^{us\ell\nu} &= \left[\bar{u}\gamma^\mu P_R s\right]\left[\bar{\ell}\gamma_\mu P_L \nu\right], \\
\mathcal{O}_{S,L,L}^{us\ell\nu} &= \left[\bar{u} P_L s\right]\left[\bar{\ell} P_L \nu\right], & \mathcal{O}_{S,R,L}^{us\ell\nu} &= \left[\bar{u} P_R s\right]\left[\bar{\ell} P_L \nu\right], \\
\mathcal{O}_{T,L}^{us\ell\nu} &= \left[\bar{u}\sigma^{\mu\nu} s\right]\left[\bar{\ell}\sigma_{\mu\nu} P_L \nu\right].
\end{aligned} \tag{4.7}$$

The operators for $K^- \to \ell^-\bar{\nu}$ in equivalence to equation 4.5 are

$$\begin{aligned}
\mathcal{O}_{V,L,R}^{us\ell\nu} &= \left[\bar{u}\gamma^\mu P_L s\right]\left[\bar{\ell}\gamma_\mu P_R \nu\right], & \mathcal{O}_{V,R,R}^{us\ell\nu} &= \left[\bar{u}\gamma^\mu P_R s\right]\left[\bar{\ell}\gamma_\mu P_R \nu\right], \\
\mathcal{O}_{S,L,R}^{us\ell\nu} &= \left[\bar{u} P_L s\right]\left[\bar{\ell} P_R \nu\right], & \mathcal{O}_{S,R,R}^{us\ell\nu} &= \left[\bar{u} P_R s\right]\left[\bar{\ell} P_R \nu\right], \\
\mathcal{O}_{T,R}^{us\ell\nu} &= \left[\bar{u}\sigma^{\mu\nu} s\right]\left[\bar{\ell}\sigma_{\mu\nu} P_R \nu\right].
\end{aligned} \tag{4.8}$$

From these operators for $K^- \to \ell^-\bar{\nu}$, the operators contributing to $\ell^- \to \nu K^-$ are constructed by computing their Hermitian conjugate. For example,

$$\begin{aligned}
\mathcal{O}_{S,L,L}^{us\ell\nu,\dagger} &= \left(\left[\bar{u} P_L s\right]\left[\bar{\ell} P_L \nu\right]\right)^\dagger \\
&= \left[\bar{s} P_L^\dagger u\right]\left[\bar{\nu} P_L dagger \ell\right] \\
&= \left[\bar{s} P_R u\right]\left[\bar{\nu} P_R \ell\right].
\end{aligned} \tag{4.9}$$

Similarly, the other $\ell^- \to \nu K^-$ operators can be found, being

$$\begin{aligned}
\mathcal{O}_{V,L,L}^{us\ell\nu,\dagger} &= \left[\bar{s}\gamma^\mu P_L u\right]\left[\bar{\nu}\gamma_\mu P_L \ell\right], & \mathcal{O}_{V,R,L}^{us\ell\nu,\dagger} &= \left[\bar{s}\gamma^\mu P_R u\right]\left[\bar{\nu}\gamma_\mu P_L \ell\right], \\
\mathcal{O}_{S,L,L}^{us\ell\nu,\dagger} &= \left[\bar{s} P_R u\right]\left[\bar{\nu} P_R \ell\right], & \mathcal{O}_{S,R,L}^{us\ell\nu,\dagger} &= \left[\bar{s} P_L u\right]\left[\bar{\nu} P_R \ell\right], \\
\mathcal{O}_{T,L}^{us\ell\nu,\dagger} &= \left[\bar{s}\sigma^{\mu\nu} u\right]\left[\bar{\nu}\sigma_{\mu\nu} P_R \ell\right],
\end{aligned} \tag{4.10}$$

for only left-handed neutrinos. Adding the option of right-handed neutrinos again, we find

$$\begin{aligned}
\mathcal{O}_{V,L,R}^{us\ell\nu,\dagger} &= \left[\bar{s}\gamma^\mu P_L u\right]\left[\bar{\nu}\gamma_\mu P_R \ell\right], & \mathcal{O}_{V,R,R}^{us\ell\nu,\dagger} &= \left[\bar{s}\gamma^\mu P_R u\right]\left[\bar{\nu}\gamma_\mu P_R \ell\right], \\
\mathcal{O}_{S,L,R}^{us\ell\nu,\dagger} &= \left[\bar{s} P_R u\right]\left[\bar{\nu} P_L \ell\right], & \mathcal{O}_{S,R,R}^{us\ell\nu,\dagger} &= \left[\bar{s} P_L u\right]\left[\bar{\nu} P_L \ell\right], \\
\mathcal{O}_{T,R}^{us\ell\nu,\dagger} &= \left[\bar{s}\sigma^{\mu\nu} u\right]\left[\bar{\nu}\sigma_{\mu\nu} P_L \ell\right].
\end{aligned} \tag{4.11}$$

Since $B^- \to \ell^-\bar{\nu}$ can happen through different interactions than $\ell^- \to K^-\nu$, the two operator sets must be used independently.

4.2 Decay constants

As explained in section 2.6, decay constants are used to describe semileptonic decays of hadrons. In the case of background process I, two decay constants are needed: f_B for B^- and f_K for K^-. The

decay constant of the B^- meson is defined as

$$\langle 0|\, \bar{u}\gamma_\mu\gamma^5 b\, |B^-(p)\rangle = if_B p_\mu\,, \tag{4.12}$$

in which p_μ is the momentum of the B^- meson. Going beyond the SM, the left-hand side of this equation can take several forms. Therefore, several expressions in terms of this decay constant are needed. Since the B^- meson is a pseudoscalar particle, the above definition applies, since

$$\langle 0|\, \bar{u}\gamma_\mu b\, |B^-(p)\rangle = 0\,. \tag{4.13}$$

Therefore, this definition can easily be translated to a right-handed and a left-handed version, for which the operators are given in equation 2.2, being

$$\begin{aligned} \langle 0|\, \bar{u}\gamma_\mu P_L b\, |B^-(p)\rangle &= \frac{-if_B p_\mu}{2}\,, \\ \langle 0|\, \bar{u}\gamma_\mu P_R b\, |B^-(p)\rangle &= \frac{if_B p_\mu}{2}\,. \end{aligned} \tag{4.14}$$

For the scalar operators $\langle 0|\, \bar{u}\underset{R}{P_L} b\, |B^-(p)\rangle$, a different formulation of this definition is needed. This formulation is found using the Dirac equation. Spinors obey the Dirac equation in the following form

$$\begin{aligned} 0 = (\not{p} - m)u(p) &= \bar{u}(p)(\not{p} - m) \\ = (\not{p} + m)v(p) &= \bar{v}(p)(\not{p} + m)\,, \end{aligned} \tag{4.15}$$

where $u(p)$ represents an incoming particle, $\bar{u}(p)$ an outgoing particle, $v(p)$ an outgoing antiparticle, and $\bar{v}(p)$ an incoming antiparticle.[18] Using this form of the Dirac equation, we find

$$\langle 0|\, i\partial^\mu \left(\bar{u}(x)\gamma_\mu\gamma_5 b(x)\right) |B^-(p)\rangle = -(m_b + m_u)\, \langle 0|\, \bar{u}\gamma_5 b\, |B^-(p)\rangle\,, \tag{4.16}$$

where m_b and m_u are the masses of respectively the b and the u quarks. On the other hand, definition 4.12 is used to find

$$\begin{aligned} \langle 0|\, i\partial^\mu(\bar{u}(x)\gamma_\mu\gamma^5 b(x))\, |B^-(p)\rangle &= p^\mu\, \langle 0|\, \bar{u}\gamma_\mu\gamma^5 b\, |B^-(p)\rangle \\ &= if_B p^\mu p_\mu \\ &= if_B M_B^2\,, \end{aligned} \tag{4.17}$$

where M_B is the mass of the B meson. Combining equations 4.16 and 4.17 gives our desired result of a scalar definition, in the same shape as equation 4.12, being

$$\begin{aligned} \langle 0|\, \bar{u}P_L b\, |B^-(p)\rangle &= \frac{if_B M_B^2}{2(m_b + m_u)}\,, \\ \langle 0|\, \bar{u}P_R b\, |B^-(p)\rangle &= \frac{-if_B M_B^2}{2(m_b + m_u)}\,. \end{aligned} \tag{4.18}$$

These are all the expressions in terms of f_B needed to do the beyond-the-SM analysis. Since the B^- meson as well as the kaon are pseudoscalars, the tensor current vanishes. In equivalence to

equation 4.12, the Kaon decay constant is defined as

$$\langle 0|\, \bar{u}\gamma_\mu\gamma_5 s\, |K^-(k)\rangle = i f_K k_\mu\,, \tag{4.19}$$

in which k_μ is the momentum of the Kaon. Applying Hermitian conjugation here to get the decay constant for Kaon creation, we get

$$\begin{aligned}\langle K^-(k)|\, \bar{s}\gamma_\mu P_L u\, |0\rangle &= i\frac{f_K}{2}k_\mu\,,\\ \langle K^-(k)|\, \bar{s}\gamma_\mu P_R u\, |0\rangle &= -i\frac{f_K}{2}k_\mu\,.\end{aligned} \tag{4.20}$$

A scalar definition will be needed and is constructed using equation 4.15, being

$$\begin{aligned}\langle K^-(k)|\, \bar{s}P_L u\, |0\rangle &= \frac{-if_K M_K^2}{2(m_s+m_u)}\,,\\ \langle K^-(k)|\, \bar{s}P_R u\, |0\rangle &= \frac{if_K M_K^2}{2(m_s+m_u)}\,,\end{aligned} \tag{4.21}$$

where m_s is the mass of the s quark.
Now that we have formulated all expressions in terms of the decay constants that we will later need, we are ready to compute the amplitude.

4.3 The Amplitude

From the two Lagrangians stated in equations 4.3 and 4.6, the amplitude for background process I is constructed. The amplitude is

$$i\mathcal{M} = i\left(\frac{4G_F}{\sqrt{2}}\right)^2 V_{ub}V_{us}^* \sum_{i,j} \mathcal{C}_i^{us\ell\nu,*}\mathcal{C}_j^{ub\ell\nu}\mathcal{M}_{ij}\frac{i}{Q^2 - m_\ell^2 + i m_\ell \Gamma_\ell}\,. \tag{4.22}$$

Here Γ_ℓ is the total decay width of the propagating charged lepton ℓ, Q the momentum of the charged lepton ℓ, m_ℓ its mass, and

$$\mathcal{M}_{ij} = \sum_{\ell\text{ spin}} \langle \nu(q_1)K^-(k)|\, \mathcal{O}_i^{us\ell\nu,\dagger}\, |\ell^-(Q)\rangle \langle \ell^-(Q)\bar{\nu}(q_2)|\, \mathcal{O}_j^{ub\ell\nu}\, |B^-(p)\rangle\,. \tag{4.23}$$

Since there are ten operators for each decay, and all options need to be combined, there are a hundred different terms in this combination. However, many of them are very similar in structure, while others vanish.
Let us first look at the SM case, using operators $\mathcal{O}_{V_L,L}^{ub\ell\nu}$ and $\mathcal{O}_{V_L,L}^{us\ell\nu,\dagger}$. The matrix element then becomes

$$\begin{aligned}\mathcal{M}_{V_{L,L}V_{L,L}} = \sum_{\ell\text{ spin}} &[\bar{u}(q_1)\gamma^\alpha P_L u(Q)]\,[\bar{u}(Q)\gamma^\mu P_L v(q_2)]\\ &\langle K^-(k)|\, \bar{s}\gamma_\alpha P_L u\, |0\rangle \langle 0|\, \bar{u}\gamma_\mu P_L b\, |B^-(p)\rangle\end{aligned} \tag{4.24}$$

Using the decay constants as discussed in section 4.2, the hadronic part of the matrix element becomes

$$\mathcal{M}_{V_{L,L}V_{L,L}} = \sum_{\ell \text{ spin}} \frac{(if_K)(-if_B)}{4} \left[\bar{u}(q_1)\gamma^\alpha P_L u(Q)\right] \left[\bar{u}(Q)\gamma^\mu P_L v(q_2)\right] k_\alpha p_\mu \,. \tag{4.25}$$

From there on, we make use of momentum conservation, implying $p^\mu = Q^\mu + q_2^\mu$ and $k^\mu = Q^\mu - q_1^\mu$. Subsequently the Diraq equation 4.15 is needed. When assuming the mass of the neutrinos is zero, it follows from applying the Dirac equation to the external fermions that the terms which involve $\not{q}_1$ or $\not{q}_2$ vanish, while the mass of the lepton appears in terms which involve $\not{Q}$. From this follows that

$$\begin{aligned}
\mathcal{M}_{V_{L,L}V_{L,L}} &= \frac{f_K f_B}{4} \sum_{\ell \text{ spin}} \left[\bar{u}(q_1)\not{k} P_L u(Q)\right] \left[\bar{u}(Q)\not{p} P_L v(q_2)\right] \\
&= \frac{f_K f_B}{4} \sum_{\ell \text{ spin}} \left[\bar{u}(q_1) P_R (\not{Q} - \not{q}_1) u(Q)\right] \left[\bar{u}(Q)(\not{Q} + \not{q}_2) P_L v(q_2)\right] \\
&= \frac{f_K f_B}{4} \sum_{\ell \text{ spin}} \left[\bar{u}(q_1) P_R m_\ell u(Q)\right] \left[\bar{u}(Q) m_\ell P_L v(q_2)\right] \,.
\end{aligned} \tag{4.26}$$

In general, while computing unpolarized cross sections one encounters the polarization sums [18]

$$\begin{aligned}
\sum_{\text{spin}} u(p)\,\bar{u}(p) &= \not{p} + m \,, \\
\sum_{\text{spin}} v(p)\,\bar{v}(p) &= \not{p} - m \,.
\end{aligned} \tag{4.27}$$

Using this, one finds two terms. Since $P_L P_R = 0$, either the contribution of $\not{p}$ or m will vanish. This is the last ingredient needed for the SM amplitude, concluding that

$$\mathcal{M}_{V_{L,L}V_{L,L}} = \frac{f_K f_B}{4} m_\ell^2 \left[\bar{u}(q_1) P_R \not{Q} P_L v(q_2)\right] \,. \tag{4.28}$$

Using the operators with left-handed neutrinos only, equation sets 4.4 and 4.10, all amplitudes simplify in a very similar way. The operator with index T does not contribute since its hadronic matrix element with pseudoscalar hadrons vanishes. The simplification of the spinor parts of the other operators follows exactly the same pattern, causing the result to differ only in constants. The results can be grouped into categories because applying a different chirality projection operator in the hadronic part changes only the sign of the result. The amplitudes then read

$$\mathcal{M}_{V_{\lambda_1,L}V_{\lambda_2,L}} = +G \frac{f_K f_B}{4} m_\ell^2 \left[\bar{u}(q_1) P_R \not{Q} P_L v(q_2)\right] \,, \tag{4.29}$$

$$\mathcal{M}_{S_{\lambda_1,L}S_{\lambda_2,L}} = -G \frac{f_K f_B}{4} \frac{M_K^2}{m_s + m_u} \frac{M_B^2}{m_b + m_u} \left[\bar{u}(q_1) P_R \not{Q} P_L v(q_2)\right] \,, \tag{4.30}$$

$$\mathcal{M}_{S_{\lambda_1,L}V_{\lambda_2,L}} = -G \frac{f_K f_B}{4} \frac{M_B^2}{m_b + m_u} m_\ell \left[\bar{u}(q_1) P_R \not{Q} P_L v(q_2)\right] \,, \tag{4.31}$$

$$\mathcal{M}_{V_{\lambda_1,L}S_{\lambda_2,L}} = +G \frac{f_K f_B}{4} \frac{M_K^2}{m_s + m_u} m_\ell \left[\bar{u}(q_1) P_R \not{Q} P_L v(q_2)\right] \,, \tag{4.32}$$

with

$$G = +1 \;\text{ if }\; \lambda_1\lambda_2 = \text{LL or RR}\,, \tag{4.33}$$

$$G = -1 \;\text{ if }\; \lambda_1\lambda_2 = \text{LR or RL}\,. \tag{4.34}$$

Adding the operator sets containing right-handed projection operators in the leptonic current, from equation sets 4.5 and 4.11, a different pattern appears. Again, using only the two right-handed equation sets 4.5 and 4.11 gives a set of matrix elements that differ only by constants. As before, the operator with index T does not contribute because its hadronic matrix element with pseudoscalar hadrons vanishes. Since the calculation is done using the same steps as for the SM matrix element, only the result is shown. The non-vanishing amplitudes are

$$\mathcal{M}_{V_{\lambda_1,R}V_{\lambda_2,R}} = +G\,\frac{f_K f_B}{4} m_\ell^2\,[\bar{u}(q_1)P_L \not{Q} P_R v(q_2)]\;, \tag{4.35}$$

$$\mathcal{M}_{S_{\lambda_1,R}S_{\lambda_2,R}} = -G\,\frac{f_K f_B}{4}\,\frac{M_K^2}{m_s+m_u}\,\frac{M_B^2}{m_b+m_u}\,[\bar{u}(q_1)P_L \not{Q} P_R v(q_2)]\;, \tag{4.36}$$

$$\mathcal{M}_{S_{\lambda_1,R}V_{\lambda_2,R}} = -G\frac{f_K f_B}{4}\,\frac{M_B^2}{m_b+m_u} m_\ell\,[\bar{u}(q_1)P_L \not{Q} P_R v(q_2)]\;, \tag{4.37}$$

$$\mathcal{M}_{V_{\lambda_1,R}S_{\lambda_2,R}} = +G\frac{f_K f_B}{4}\,\frac{M_K^2}{m_s+m_u} m_\ell\,[\bar{u}(q_1)P_L \not{Q} P_R v(q_2)]\;. \tag{4.38}$$

The constant part stays unchanged compared to the previous situation, but the part in the brackets containing the spinors is slightly different.
It all gets more interesting if one looks at combinations of the two operator sets. Still, the operator with index T does not contribute. Using 4.4 and 4.11, the non-vanishing amplitudes become

$$\mathcal{M}_{V_{\lambda_1,L}V_{\lambda_2,R}} = +G\,\frac{f_K f_B}{4} m_\ell^3\,[\bar{u}(q_1)P_L v(q_2)]\;, \tag{4.39}$$

$$\mathcal{M}_{S_{\lambda_1,L}S_{\lambda_2,R}} = -G\,\frac{f_K f_B}{4}\,\frac{M_K^2}{m_s+m_u}\,\frac{M_B^2}{m_b+m_u} m_\ell\,[\bar{u}(q_1)P_L v(q_2)]\;, \tag{4.40}$$

$$\mathcal{M}_{S_{\lambda_1,L}V_{\lambda_2,R}} = -G\frac{f_K f_B}{4}\,\frac{M_B^2}{m_b+m_u} m_\ell^2\,[\bar{u}(q_1)P_L v(q_2)]\;, \tag{4.41}$$

$$\mathcal{M}_{V_{\lambda_1,L}S_{\lambda_2,R}} = +G\frac{f_K f_B}{4}\,\frac{M_K^2}{m_s+m_u} m_\ell^2\,[\bar{u}(q_1)P_L v(q_2)]\;. \tag{4.42}$$

Similarly, the nonvanishing amplitudes that emerge when using operator sets 4.5 and 4.10 are

$$\mathcal{M}_{V_{\lambda_1,R}V_{\lambda_2,L}} = +G\,\frac{f_K f_B}{4} m_\ell^3\,[\bar{u}(q_1)P_R v(q_2)]\;, \tag{4.43}$$

$$\mathcal{M}_{S_{\lambda_1,R}S_{\lambda_2,L}} = -G\,\frac{f_K f_B}{4}\,\frac{M_K^2}{m_s+m_u}\,\frac{M_B^2}{m_b+m_u} m_\ell\,[\bar{u}(q_1)P_R v(q_2)]\;, \tag{4.44}$$

$$\mathcal{M}_{S_{\lambda_1,R}V_{\lambda_2,L}} = -G\frac{f_K f_B}{4}\,\frac{M_B^2}{m_b+m_u} m_\ell^2\,[\bar{u}(q_1)P_R v(q_2)]\;, \tag{4.45}$$

$$\mathcal{M}_{V_{\lambda_1,R}S_{\lambda_2,L}} = +G\frac{f_K f_B}{4}\,\frac{M_K^2}{m_s+m_u} m_\ell^2\,[\bar{u}(q_1)P_R v(q_2)]\;. \tag{4.46}$$

These are all 64 $\mathcal{M}_{ij}$ contained in equation 4.22, all carrying their own Wilson coefficients. The total amplitude requires adding all these contributions.

4.4 The Amplitude Squared

In the previous section all amplitudes are calculated and simplified. There were a hundred terms in total; however, only 64 of them were nonzero. These amplitudes are grouped into four categories, in which the amplitudes only differ by constants. Since the square of constants is computed trivially, in this section the focus will be on the spinor part of the amplitudes. Since the four different spinor parts need to be multiplied by four different complex conjugates, sixteen computations are needed. However, we will see that many contributions vanish. As previously, the first part of this calculation will be on the SM part of the amplitude squared.
As found in equation 4.28, the spinor part S of the SM matrix element reads

$$S_{L,L} = [\bar{u}(q_1)\not{Q}P_L v(q_2)] \ , \tag{4.47}$$

where the indices on the S indicate the leptonic current of the operator set.
For the spin-averaged amplitude squared, $S_{L,L}$ must be multiplied by the complex conjugate of this SM part of the amplitude and the spin sum must be taken, giving

$$\left\langle S_{L,L} S_{L,L}^{\dagger} \right\rangle = \sum_{\text{spin}} [\bar{u}(q_1)\not{Q}P_L v(q_2)] \ [\bar{v}(q_2)P_R \not{Q} u(q_1)] \ . \tag{4.48}$$

Here Casimir's Trick comes in handy, to perform a trace transformation using products of Dirac matrices. Subsequently the Dirac equation 4.27 is used, again assuming a massless neutrino. The spinor part of the amplitude squared then becomes

$$\begin{aligned} \left\langle S_{L,L} S_{L,L}^{\dagger} \right\rangle &= \mathsf{Tr}\left[u(q_1)\bar{u}(q_1)\not{Q}P_L v(q_2)\bar{v}(q_2)\not{Q}P_L\right] \\ &= \mathsf{Tr}\left[\not{q}_1\not{Q}P_L\not{q}_2\not{Q}P_L\right] \\ &= \frac{1}{2} q_{1\alpha} q_{2\beta} Q_\mu Q_\nu \mathsf{Tr}\left[\gamma^\alpha\gamma^\mu\gamma^\beta\gamma^\nu\left(1-\gamma^5\right)\right] \ . \end{aligned} \tag{4.49}$$

The trace identities of γ matrices is listed in [18], providing a Levi-Civita tensor along with several Minkowski metrics. Because the Levi-Civita tensor is defined to be totally antisymmetric, it can only be nonvanishing when contracted with four independent four-vectors. Here, the Levi-Civita tensor is contracted with Q twice, implying that it does not contribute. This leads to

$$\begin{aligned} \left\langle S_{L,L} S_{L,L}^{\dagger} \right\rangle &= 2 q_{1\alpha} q_{2\beta} Q_\mu Q_\nu \left(\eta^{\alpha\mu}\eta^{\beta\nu} - \eta^{\alpha\beta}\eta^{\mu\nu} + \eta^{\alpha\nu}\eta^{\beta\mu} + i\epsilon^{\alpha\mu\beta\nu}\right) \\ &= 4 q_1 \cdot Q \, q_2 \cdot Q - 2 q_1 \cdot q_2 \, Q^2 \, . \end{aligned} \tag{4.50}$$

The expressions needed to find the required dot products are listed in Appendix A.3. For the dot product of the two neutrino momenta, a Lorentz boost is required since they are defined in two different frames: the rest frame of the B^- meson and the rest frame of the mediating lepton. Using

the definitions given in the appendix, the required dot products for this expression are

$$q_1 \cdot Q = |\vec{k}| m_\ell \,, \tag{4.51}$$

$$q_2 \cdot Q = |\vec{Q}| M_B \,, \tag{4.52}$$

$$q_1 \cdot q_2 = \frac{|\vec{Q}||\vec{k}| M_B}{m_\ell}(1 - \cos\theta) \,, \tag{4.53}$$

$$Q^2 = m_\ell^2 \,. \tag{4.54}$$

The final version of the spinor part of amplitude squared in the SM thus reads

$$\left\langle S_{L,L} S_{L,L}^\dagger \right\rangle = 2|\vec{Q}|\,|\vec{k}| M_B m_\ell (1 + \cos\theta) \,. \tag{4.55}$$

Now that the SM part is completed, we continue with the other spinor parts multiplied by their own complex conjugate before looking into the cross terms.
The spinor part $S_{L,R}$ of amplitudes $\mathcal{M}_{V_{\lambda,L} V_{\lambda,R}}$ multiplied by its own complex conjugate is computed similarly as in the SM case, and gives

$$\left\langle S_{L,R} S_{L,R}^\dagger \right\rangle = \sum_{\text{spin}} \left[\bar{u}(q_1) P_L v(q_2)\right] \left[\bar{v}(q_2) P_R u(q_1)\right] \,, \tag{4.56}$$

$$= \text{Tr}\left[\not{q}_1 P_L \not{q}_2\right] \,, \tag{4.57}$$

$$= 2 q_1 \cdot q_2 \,, \tag{4.58}$$

$$= q^2 \,. \tag{4.59}$$

The squares of the spinor parts $S_{R,R}$ and $S_{R,L}$ of $\mathcal{M}_{V_{\lambda,R} V_{\lambda,R}}$ and $\mathcal{M}_{V_{\lambda,R} V_{\lambda,L}}$ are exactly the same as respectively $\mathcal{M}_{V_{\lambda,L} V_{\lambda,L}}$ and $\mathcal{M}_{V_{\lambda,L} V_{\lambda,R}}$.
Now let's look at the cross terms. We will see that all combinations of different spinor parts vanish for two reasons. Firstly, due to the anticommutation of γ^5 with the Dirac matrices and that $P_L P_R = 0$, the multiplication of $S_{L,L}$ by $S_{R,R}^\dagger$ vanishes:

$$\left\langle S_{L,L} S_{R,R}^\dagger \right\rangle = \sum_{\text{spin}} \left[\bar{u}(q_1) \not{Q} P_L v(q_2)\right] \left[\bar{v}(q_2) P_L \not{Q} u(q_1)\right] \,, \tag{4.60}$$

$$= \sum_{\text{spin}} \left[\bar{u}(q_1) \not{Q} v(q_2)\right] \left[\bar{v}(q_2) P_R P_L \not{Q} u(q_1)\right] \,, \tag{4.61}$$

$$= 0 \,. \tag{4.62}$$

In a similar manner $S_{R,R} S_{L,L}^\dagger$, $S_{L,R} S_{R,L}^\dagger$, and $S_{R,L} S_{L,R}^\dagger$ vanish. Secondly, the trace of any odd number of γ matrices is zero. Therefore the multiplications $S_{L,L} S_{L,R}^\dagger$, $S_{L,L} S_{R,L}^\dagger$, $S_{R,R} S_{L,R}^\dagger$, $S_{R,R} S_{R,L}^\dagger$, as well as their complex conjugates vanish.
Although we have only four nonvanishing linearly independent terms left, the total amplitude squared is a lengthy expression. The branching ratio is computed with this expression.

4.5 Interference Between Signal and Background Process I

Before computing the branching ratio from the expression at hand, we need to know to what extent there is interference between the signal and background process I. Schematically, the process $B \to K\nu\bar{\nu}$ is described by the two subprocesses: the signal process with amplitude $\mathcal{M}_S$; and the background process I describe in this chapter, with amplitude $\mathcal{M}_{BP1}$.
Since both the initial state and the final states of both processes are identical, we have to sum their amplitudes coherently. The decay rate will then contain both processes separately, but it also has an interference term. The calculation of this interference term can be found in Appendix B. In calculation an on-shell τ is used. We will later see how this is justified. The branching ratio is proportional to

$$\begin{aligned}\frac{d\mathcal{B}}{dq^2} &\propto \left|\mathcal{M}_S(q^2) + \mathcal{M}_{BPI}(Q^2, q^2)\right|^2 \\ &= \left|\mathcal{M}_S(q^2)\right|^2 + 2\,\mathrm{Re}\left\{\mathcal{M}_S^*(q^2)\tilde{\mathcal{M}}_B(Q^2, q^2)\right\}\pi\delta(Q^2 - m_\tau^2) \\ &\quad + \left|\tilde{\mathcal{M}}_B(Q^2, q^2)\right|^2 \frac{\pi}{m_\tau\Gamma_\tau}\delta(Q^2 - m_\tau^2)\end{aligned} \tag{4.63}$$

We want to know which of these terms contributes significantly. The first term scales with G_F^2. The last term scales with $\frac{G_F^4}{G_F^2} = G_F^2$. The second term, however, scales with G_F^3. Therefore we can neglect the interference term.

4.6 The Branching Ratio

The partial branching of background process I is found using

$$d\mathcal{B} = \frac{(2\pi)^4}{2M_B\Gamma_B}\left\langle|\mathcal{M}|^2\right\rangle d\Phi_3(p; k, q_1, q_2)\,. \tag{4.64}$$

The phase space element $d\Phi_3(p; k, q_1, q_2)$ is constructed in Appendix A.3. The result reads

$$d\Phi_3(p; k, q_1, q_2) = \frac{d\cos\theta\, dQ^2}{32(2\pi)^7}\,\frac{Q^2 - M_K^2}{Q^2}\,\frac{M_B^2 - Q^2}{M_B^2}\,\Theta(M_B - E_\ell)\,\Theta(m_\ell - E_K)\,. \tag{4.65}$$

To obtain an expression for $\frac{d\mathcal{B}}{dq^2}$, we rewrite $d\mathcal{B}$ in terms of q^2 and dq^2 instead of $\cos\theta$ and $d\cos\theta$. This is done using the expression for q^2, being

$$q^2 \quad = \quad 2\frac{|\vec{Q}||\vec{k}|M_B}{m_\ell}(1 - \cos\theta). \tag{4.66}$$

Furthermore integration over Q^2 is needed. For this we use the narrow-width approximation, assuming the mediating lepton is on-shell. Since on-shell muons and electrons are too light to decay into a kaon, this implies that our mediating lepton is a τ particle. We use

$$dQ^2\frac{1}{(Q^2 - m_\tau^2)^2 + m_\tau^2\Gamma_\tau^2} \mapsto dQ^2 C \times \delta(Q^2 - m_\tau^2)\,, \tag{4.67}$$

with

$$C = \int_{-\infty}^{+\infty} dQ^2 \frac{1}{(Q^2 - m_\tau^2)^2 + m_\tau^2 \Gamma_\tau^2} = \frac{\pi}{m_\tau \Gamma_\tau}\,. \tag{4.68}$$

These two ingredients lead to the final result for this process. Defining the constants

$$R_B = \frac{M_B^2}{m_b + m_u} \tag{4.69}$$

$$R_K = \frac{M_K^2}{m_s + m_u}, \tag{4.70}$$

two matrices

$$\mathbf{M_1} = \begin{pmatrix} m_\tau^2 & -m_\tau^2 & R_B m_\tau & -R_B m_\tau \\ -m_\tau^2 & m_\tau^2 & -R_B m_\tau & R_B m_\tau \\ -R_K m_\tau & R_K m_\tau & -R_K R_B & R_K R_B \\ R_K m_\tau & -R_K m_\tau & R_K R_B & -R_K R_B \end{pmatrix}, \tag{4.71}$$

and

$$\mathbf{M_2} = \begin{pmatrix} m_\tau^2 & -m_\tau^2 & -R_K m_\tau & R_K m_\tau \\ -m_\tau^2 & m_\tau^2 & R_K m_\tau & -R_K m_\tau \\ R_B m_\tau & -R_B m_\tau & -R_K R_B & R_K R_B \\ -R_B m_\tau & R_B m_\tau & R_K R_B & -R_K R_B \end{pmatrix}, \tag{4.72}$$

the branching ratio of this process is

$$
\begin{aligned}
\frac{d\mathcal{B}}{dq^2} = &\left(\frac{4G_F}{\sqrt{2}}\right)^4 \left(\frac{f_K\, f_B}{4}\right)^2 \frac{|V_{ub}|^2|V_{us}|^2}{64\Gamma_\tau \Gamma_B M_B^3 m_\tau} \frac{1}{(2\pi)^2} \left((M_B^2 - m_\tau^2)(m_\tau^2 - M_K^2) - q^2 m_\tau^2\right) \\
&\Theta(M_B - E_\tau)\Theta(m_\tau - E_K) \\
&(C^{us\ell\nu,*}_{V_{L,L}}, C^{us\ell\nu,*}_{V_{R,L}}, C^{us\ell\nu,*}_{S_{L,L}}, C^{us\ell\nu,*}_{S_{R,L}})\mathbf{M_1} \left(C^{ub\ell\nu}_{V_{L,L}}, C^{ub\ell\nu}_{V_{R,L}}, C^{ub\ell\nu}_{S_{L,L}}, C^{ub\ell\nu}_{S_{R,L}}\right)^T \\
&(C^{*,ub\ell\nu}_{V_{L,L}}, C^{*,ub\ell\nu}_{V_{R,L}}, C^{*,ub\ell\nu}_{S_{L,L}}, C^{*,ub\ell\nu}_{S_{R,L}})\mathbf{M_2} \left(C^{us\ell\nu}_{V_{L,L}}, C^{us\ell\nu}_{V_{R,L}}, C^{us\ell\nu}_{S_{L,L}}, C^{us\ell\nu}_{S_{R,L}}\right)^T \\
+ &\left(\frac{4G_F}{\sqrt{2}}\right)^4 \left(\frac{f_K\, f_B}{4}\right)^2 \frac{|V_{ub}|^2|V_{us}|^2}{64\Gamma_\tau \Gamma_B M_B^3 m_\tau} \frac{1}{(2\pi)^2} \left((M_B^2 - m_\tau^2)(m_\tau^2 - M_K^2) - q^2 m_\tau^2\right) \\
&\Theta(M_B - E_\tau)\Theta(m_\tau - E_K) \\
&(C^{us\ell\nu,*}_{V_{L,R}}, C^{us\ell\nu,*}_{V_{R,R}}, C^{us\ell\nu,*}_{S_{L,R}}, C^{us\ell\nu,*}_{S_{R,R}})\mathbf{M_1} \left(C^{ub\ell\nu}_{V_{L,R}}, C^{ub\ell\nu}_{V_{R,R}}, C^{ub\ell\nu}_{S_{L,R}}, C^{ub\ell\nu}_{S_{R,R}}\right)^T \\
&(C^{*,ub\ell\nu}_{V_{L,R}}, C^{*,ub\ell\nu}_{V_{R,R}}, C^{*,ub\ell\nu}_{S_{L,R}}, C^{*,ub\ell\nu}_{S_{R,R}})\mathbf{M_2} \left(C^{us\ell\nu}_{V_{L,R}}, C^{us\ell\nu}_{V_{R,R}}, C^{us\ell\nu}_{S_{L,R}}, C^{us\ell\nu}_{S_{R,R}}\right)^T \\
+ &\left(\frac{4G_F}{\sqrt{2}}\right)^4 \left(\frac{f_K\, f_B}{4}\right)^2 \frac{|V_{ub}|^2|V_{us}|^2}{64\Gamma_\tau \Gamma_B M_B^3 m_\tau} \frac{1}{(2\pi)^2} q^2 m_\tau^2 \Theta(M_B - E_\tau)\Theta(m_\tau - E_K) \\
&(C^{us\ell\nu,*}_{V_{L,L}}, C^{us\ell\nu,*}_{V_{R,L}}, C^{us\ell\nu,*}_{S_{L,L}}, C^{us\ell\nu,*}_{S_{R,L}})\mathbf{M_1} \left(C^{ub\ell\nu}_{V_{L,R}}, C^{ub\ell\nu}_{V_{R,R}}, C^{ub\ell\nu}_{S_{L,R}}, C^{ub\ell\nu}_{S_{R,R}}\right)^T \\
&(C^{*,ub\ell\nu}_{V_{L,R}}, C^{*,ub\ell\nu}_{V_{R,R}}, C^{*,ub\ell\nu}_{S_{L,R}}, C^{*,ub\ell\nu}_{S_{R,R}})\mathbf{M_2} \left(C^{us\ell\nu}_{V_{L,L}}, C^{us\ell\nu}_{V_{R,L}}, C^{us\ell\nu}_{S_{L,L}}, C^{us\ell\nu}_{S_{R,L}}\right)^T \\
+ &\left(\frac{4G_F}{\sqrt{2}}\right)^4 \left(\frac{f_K\, f_B}{4}\right)^2 \frac{|V_{ub}|^2|V_{us}|^2}{64\Gamma_\tau \Gamma_B M_B^3 m_\tau} \frac{1}{(2\pi)^2} q^2 m_\tau^2 \Theta(M_B - E_\tau)\Theta(m_\tau - E_K) \\
&(C^{us\ell\nu,*}_{V_{L,R}}, C^{us\ell\nu,*}_{V_{R,R}}, C^{us\ell\nu,*}_{S_{L,R}}, C^{us\ell\nu,*}_{S_{R,R}})\mathbf{M_1} \left(C^{ub\ell\nu}_{V_{L,L}}, C^{ub\ell\nu}_{V_{R,L}}, C^{ub\ell\nu}_{S_{L,L}}, C^{ub\ell\nu}_{S_{R,L}}\right)^T \\
&(C^{*,ub\ell\nu}_{V_{L,L}}, C^{*,ub\ell\nu}_{V_{R,L}}, C^{*,ub\ell\nu}_{S_{L,L}}, C^{*,ub\ell\nu}_{S_{R,L}})\mathbf{M_2} \left(C^{us\ell\nu}_{V_{L,R}}, C^{us\ell\nu}_{V_{R,R}}, C^{us\ell\nu}_{S_{L,R}}, C^{us\ell\nu}_{S_{R,R}}\right)^T .
\end{aligned}
\tag{4.73}
$$

4.7 Analysis

In the SM, only one Wilson coefficient per part of the process is nonzero, namely $C^{ub\ell\nu}_{V_{L,L}} = 1$ for $B^- \to \tau^- \bar{\nu}$ and $C^{us\ell\nu}_{V_{L,L}} = 1$ for $\tau^- \to K^- \nu$. In this case, the partial branching ratio of the first background process $B^- \to \tau^- [\to K^- \nu] \bar{\nu}$ as a function of q^2 can be seen in Figure 4.2. The branching ratio is plotted for all physical values of q^2, which takes maximal and minimal values for $\cos\theta = -1$ to $\cos\theta = +1$. This gives a restriction for q^2 of

$$
0 \leq q^2 \leq \frac{(M_B^2 - m_\tau^2)(m_\tau^2 - M_K^2)}{m_\tau^2}. \tag{4.74}
$$

From Figure 4.2 we see that the branching ratio depends linearly on q^2. And, as q^2 approaches its upper bound, $\frac{d\mathcal{B}}{dq^2}$ approaches 0.

When exploring beyond the SM, it is convenient to choose a small set of Wilson coefficients to be

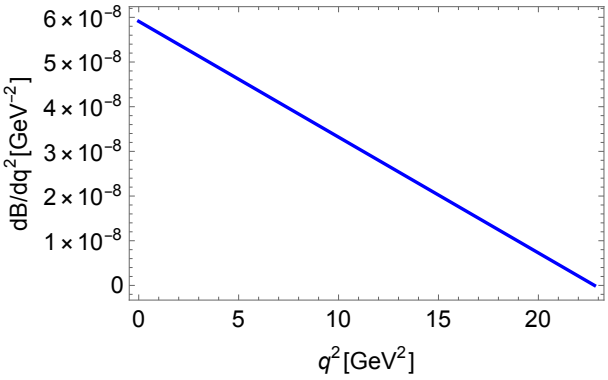

Figure 4.2 The partial branching ratio in the SM of $B^- \to \tau^-[\to K^-\nu]\bar{\nu}$, as a function of the energy of the two neutrinos q^2.

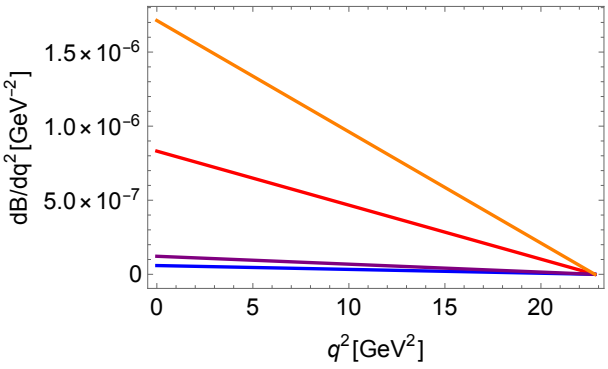

Figure 4.3 The beyond-SM partial branching ratio of $B^- \to \tau^-[\to K^-\nu]\bar{\nu}$ as a function of the energy of the two neutrinos q^2. The different lines denote a different combination of Wilson coefficients, one for $B^- \to \tau^-\bar{\nu}$ and one for $\tau^- \to K^-\nu$ to be nonzero. All others are set to zero. The blue line shows the SM contribution, with $C^{us\ell\nu}_{V_{L,L}} = C^{ub\ell\nu}_{V_{L,L}} = 1$. The purple line shows $C^{us\ell\nu}_{S_{L,L}} = C^{ub\ell\nu}_{V_{L,L}} = 1$. The red line shows $C^{us\ell\nu}_{V_{L,L}} = C^{ub\ell\nu}_{S_{L,L}} = 1$. The orange line shows $C^{us\ell\nu}_{S_{L,L}} = C^{ub\ell\nu}_{S_{L,L}} = 1$.

nonzero while setting the others to zero. In this way, the contribution of a certain operator can be compared clearly with the SM. We describe four different cases. The first case is the different combinations of Wilson coefficients of the first sets, with left-handed leptonic current: sets 4.4 and 4.10. The next case is the combinations with only Wilson coefficients of the second sets, with right-handed leptonic current: sets 4.5 and 4.11. Subsequently, the two sets are combined: first with only vector currents, and then a combination of a vector current and a scalar current.

Let us first look at the contributions with left-handed neutrinos only. In Figure 4.3 the branching ratios are shown where specific sets of Wilson coefficients are set to 1, setting all others to 0. The chirality of the hadronic current does not have an effect on the branching ratio, because the quantum numbers of the involved hadrons determine the chiral structure of the current and therefore only combinations with Wilson coefficients belonging to left-handed chirality of the hadronic current are shown. Figure 4.3 shows that the contributions all have the same shape; they depend linearly on q^2, and as q^2 approaches its upper bound, $\frac{d\mathcal{B}}{dq^2}$ approaches 0. However, the slope is different. The suppression of the contributions with Wilson coefficients C_V relative to the contributions with Wilson coefficients C_S is due to the proportionality of the C_V contributions to m_τ. These contributions are therefore chirally suppressed compared to the C_S contributions.

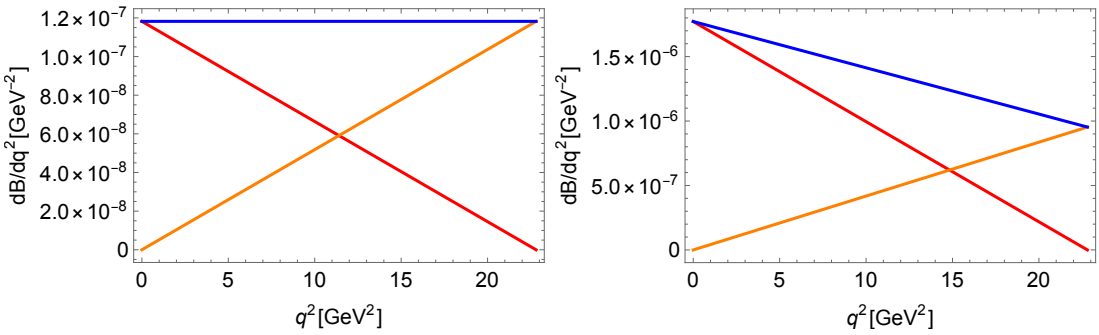

(a) The only nonzero coefficients are $C^{us\ell\nu}_{V_L,L} = C^{ub\ell\nu}_{V_L,L} = C^{us\ell\nu}_{V_L,R} = C^{ub\ell\nu}_{V_L,R} = 1$.

(b) The only nonzero coefficients are $C^{us\ell\nu}_{V_L,L} = C^{ub\ell\nu}_{V_L,L} = C^{us\ell\nu}_{S_L,R} = C^{ub\ell\nu}_{S_L,R} = 1$.

Figure 4.4 In both figures, the blue line represents the branching ratio of $B^- \to \tau^-[\to K^-\nu]\bar{\nu}$, with the given sets of Wilson coefficients. The red line represents the terms seen before in Figure 4.3, whereas the orange line represents the cross terms. The blue line is formed by these terms added.

The Wilson coefficients can have any value, positive or negative. If the SM were not the whole story in this process, the slope of the decay rate of this process would therefore be changed by the contributions beyond the SM. However, the shape would stay the same.

Using right-handed leptonic operators only, we find exactly the same branching ratios as in Figure 4.3. For example, a single set of Wilson coefficients with right-handed leptonic current being nonzero, like $C^{us\ell\nu}_{V_L,R} = C^{ub\ell\nu}_{V_L,R} = 1$, gives exactly the same behavior as in the SM case, shown in 4.2. However, cross terms appear if one allows nonzero Wilson coefficients carrying different leptonic currents. This happens if the propagating lepton flips chirality between the first and the second interaction. In Figure 4.4 the decay width is shown with nonzero Wilson coefficients of left-handed as well as right-handed leptonic current.

The interaction term modifies the shape of the branching ratio significantly since this term grows with q^2. If the interaction with left-handed leptonic current has an equal interaction strength to the interaction with right-handed leptonic current, such as in Figure 4.4a, the branching ratio is independent of q^2. If the two interactions are unequal but nonzero as in Figure 4.4b, the branching ratio decreases with q^2, but still is nonzero when q^2 reaches its maximum value.

4.8 The Shape

In the experimental analysis carried out by Belle II, the SM signal as well as background process I are fitted simultaneously, retaining a signal-only result. To do this, they use the normalized shape of the branching ratio as a function of q^2.

To analyze the shape of the branching ratio, we distinguish two situations. When all nonzero Wilson coefficients are of the operators with the same leptonic current, we observe only one possible shape of the branching ratio. The shape is shown in Figure 4.5a. It runs linearly from a maximum branching ratio at $q^2 = 0$ to 0 at the maximum value for q^2. This maximum value is defined in equation 4.74.

When nonzero Wilson coefficients belonging to operators with different chirality of the leptonic

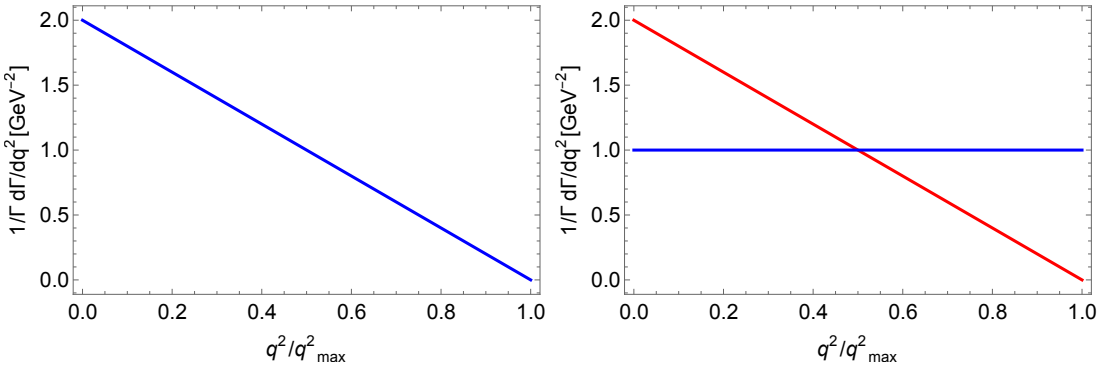

(a) The normalized shape of the branching ratio where all nonzero Wilson coefficients belong to operators with the same leptonic current. The blue line shows the only possible shape.

(b) The normalized shape of the branching ratio where Wilson coefficients belonging to different leptonic currents are nonzero. The blue and the red lines are possible shapes, as well as all straight lines in between.

Figure 4.5 The normalized shapes of the branching ratio of $B^- \to \tau^-[K^-\nu]\bar{\nu}$ in SM and beyond. Here q^2 runs from 0 to its maximum value.

current are taken into consideration, the branching ratio as a function of q^2 has a different shape. Figure 4.5b shows two branching ratios where nonzero Wilson coefficients of different leptonic current are taken into consideration. The blue, horizontal line is obtained by choosing the Wilson coefficients such that the interaction strength of the left-handed leptonic current is equal to the interaction strength of the right-handed leptonic current. The descending red line is obtained by setting one of the Wilson coefficients to zero. There is a set of Wilson coefficients for obtaining all lines in between.

In the SM, only a left-handed leptonic current is allowed. Therefore the analyses of Belle II are done using the shape of Figure 4.5a. Since the shape is significantly different in a beyond-the-SM case where right-handed leptonic current is allowed, the analyses of the signal could yield a different result if this shape is taken into account. Therefore the analyses need to be redone in order to take new physics in the lepton mediated $B^- \to K^-\nu\bar{\nu}$ into account.

4.9 The Possible Contributions

Apart from the branching ratio and its shape, equation 4.73 contains information about the possible Wilson coefficients for gaining a certain branching ratio. Since all different coefficients contribute positively to the branching ratio, there are various combinations of coefficients that have the same branching ratio. To analyze this, the differential branching ratio is integrated and then used.

In Figures 4.6, different combinations of Wilson coefficients are shown. For practical purposes, the nonzero Wilson coefficients are chosen to be the same for both parts of the process. In Subfigure 4.6a the branching ratio in terms of $C_{S_{L,L}}$ is plotted against the SM coefficient $C_{V_{L,L}}$. In Subfigure 4.6b $C_{V_{L,R}}$ is plotted against the SM coefficient $C_{V_{L,L}}$. In Subfigure 4.6c $C_{S_{L,R}}$ is plotted against the SM coefficient $C_{V_{L,L}}$.

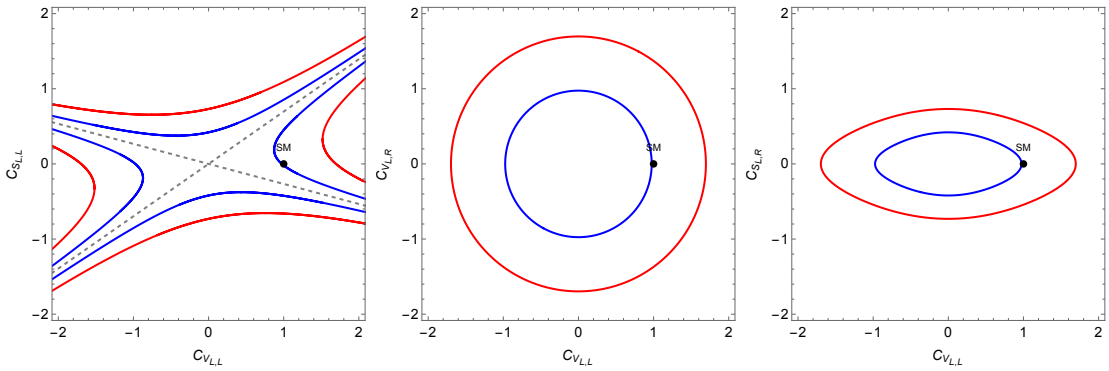

(a) $C_{V_{L,L}}$ plotted against $C_{S_{L,L}}$. *(b)* $C_{V_{L,L}}$ plotted against $C_{V_{L,R}}$. *(c)* $C_{V_{L,L}}$ plotted against $C_{S_{L,R}}$.

Figure 4.6 The combinations of Wilson coefficients for which the branching ratio has the predicted SM value are in blue. The combination of Wilson coefficients for which the branching ratio of this background process reaches the same value as the predicted branching ratio for the signal in the SM are in red. The black dot denotes the Wilson coefficients predicted by the SM.

In all figures, in blue the values of the Wilson coefficients are shown for which the branching ratio is $\mathcal{B} = 6.09 \cdot 10^{-7}$ GeV, the value of the predicted branching ratio in the SM. In the SM, only $C_{V_{L,L}} = 1$ for both processes; all others are zero. The black dot denotes the Wilson coefficients predicted by the SM.

The red line denotes the values of the Wilson coefficients for which the branching ratio is $\mathcal{B} = 5.58 \cdot 10^{-6}$ GeV, the value of the predicted branching ratio of the signal in the SM. For these values of the Wilson coefficients, the branching ratio of background process I would reach the same values as the branching ratio of the signal process predicted by the SM.

We see in all figures that various combinations of Wilson coefficients are providing us with the same branching ratio. Also, a small change of one of the Wilson coefficients beyond the SM can lead to the Background I contribution being as high as the signal contribution.

Chapter 5

Background process II: $B^- \to \pi^0 \ell^- \left[\to K^- \nu\right] \bar{\nu}$

At first glance $B^- \to \pi^0 \ell^- [\to K^- \nu] \bar{\nu}$ does not look like a background process to the signal because there is an additional particle in the final state. However, considering that the pion in this process is uncharged and long-lived, it can easily be missed in a detector. On account of the fact that the neutrinos are indirectly detected as missing energy, the momentum of the pion can be interpreted as part of the neutrino momentum and therefore the process can be misinterpreted as $B^- \to K^- \nu\bar{\nu}$. Since the background would not be a background if the detection efficiency were perfect, background process II is called a reducible background. A diagram of the process subject of this chapter can be viewed in Figure 5.1.
To analyze this process, we define the momenta of the process as

$$B^-(p) \to W^-(P) \left[\to \ell^-(Q) \left[\to K^-(k)\nu(q_1)\right] \bar{\nu}(q_2)\right] \pi^0(p') \,. \tag{5.1}$$

Since the decay constants relevant for this process are defined in terms of a mediating boson, we include this boson in our definition of the kinematics of the process. In the SM, this boson is the W^-; however, beyond the SM this could be a different mediator particle. Additionally, we define $q^2_{lost} = (q_1 + q_2 + p')^2$, the momentum of the neutrinos and the pion added, then squared. This is the momentum that is missed in the detector. The expression for q^2_{lost} can be found in equation A.44 in Appendix A.4.
Similarly as for $B^- \to \ell^- [\to K^- \nu] \bar{\nu}$, the final aim is to calculate the branching ratio of the lepton-mediated cascade $B^- \to \pi^0 K^- \nu\bar{\nu}$, in the SM and beyond. Since the final aim is the same, the approach in this chapter is the same as in chapter 4. We will start with the Lagrangian of this process, shaping the operators and the decay constants used into the right form. The partial decay rate of this process is

$$d\mathcal{B} = \frac{(2\pi)^4}{2M_B\Gamma_B} \left\langle |\mathcal{M}|^2 \right\rangle d\Phi_4(p; p', k, q_1, q_2) \,, \tag{5.2}$$

therefore the amplitude $\mathcal{M}$ and its square $\left\langle |\mathcal{M}|^2 \right\rangle$ are computed. Deriving the phase space element $d\Phi_4(p; p', k, q_1, q_2)$ and the decay rate are beyond the scope of this thesis, but a sketch of how to proceed with this process is given.

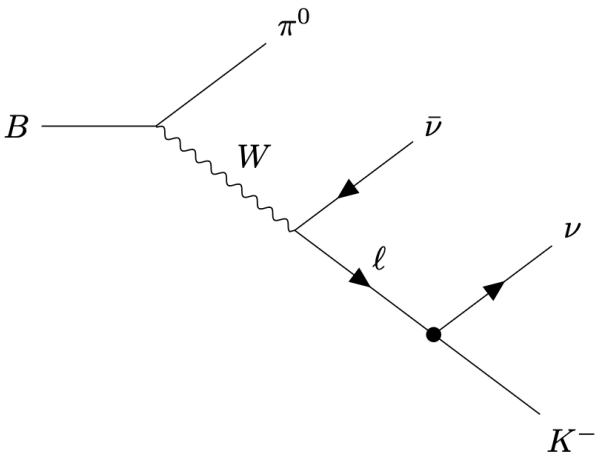

Figure 5.1 The Feynman diagram of background process II: $B^- \to \pi^0 \ell^- [\to K^- \nu] \bar{\nu}$, in a weak effective theory. The W represents any mediator particle.

5.1 The Operators

Just as for background process I, background process II is a cascade, and the two parts of the process are described separately first and used as the first ingredients for the differential decay width. Since the change in the particle content is the same in both processes, the operators are exactly the same as for background process I.
For the process $B^- \to \pi^0 \ell^-$ we use the following effective Lagrangian, as introduced in chapter 3:

$$\mathcal{L}^{ub\ell\nu} = \frac{4G_F}{\sqrt{2}} V_{ub} \sum_i \mathcal{C}_i^{ub\ell\nu} \mathcal{O}_i^{ub\ell\nu} \,. \tag{5.3}$$

We divide the operators in two sets, being

$$\begin{aligned} \mathcal{O}_{V,L,L}^{ub\ell\nu} &= \left[\bar{u}\gamma^\mu P_L b\right] \left[\bar{\ell}\gamma_\mu P_L \nu\right], & \mathcal{O}_{V,R,L}^{ub\ell\nu} &= \left[\bar{u}\gamma^\mu P_R b\right] \left[\bar{\ell}\gamma_\mu P_L \nu\right], \\ \mathcal{O}_{S,L,L}^{ub\ell\nu} &= \left[\bar{u} P_L b\right] \left[\bar{\ell} P_L \nu\right], & \mathcal{O}_{S,R,L}^{ub\ell\nu} &= \left[\bar{u} P_R b\right] \left[\bar{\ell} P_L \nu\right], \\ \mathcal{O}_{T,L}^{ub\ell\nu} &= \left[\bar{u}\sigma^{\mu\nu} b\right] \left[\bar{\ell}\sigma_{\mu\nu} P_L \nu\right], \end{aligned} \tag{5.4}$$

with only left-handed neutrinos, and

$$\begin{aligned} \mathcal{O}_{V,L,R}^{ub\ell\nu} &= \left[\bar{u}\gamma^\mu P_L b\right] \left[\bar{\ell}\gamma_\mu P_R \nu\right], & \mathcal{O}_{V,R,R}^{ub\ell\nu} &= \left[\bar{u}\gamma^\mu P_R b\right] \left[\bar{\ell}\gamma_\mu P_R \nu\right], \\ \mathcal{O}_{S,L,R}^{ub\ell\nu} &= \left[\bar{u} P_L b\right] \left[\bar{\ell} P_R \nu\right], & \mathcal{O}_{S,R,R}^{ub\ell\nu} &= \left[\bar{u} P_R b\right] \left[\bar{\ell} P_R \nu\right], \\ \mathcal{O}_{T,R}^{ub\ell\nu} &= \left[\bar{u}\sigma^{\mu\nu} b\right] \left[\bar{\ell}\sigma_{\mu\nu} P_R \nu\right], \end{aligned} \tag{5.5}$$

where right-handed neutrinos are added to the system.
For the second half of the process, $\ell^- \to K^- \nu$, the following effective Lagrangian is used:

$$\mathcal{L}^{us\ell\nu} = \frac{4G_F}{\sqrt{2}} V_{us} \sum_i \mathcal{C}_i^{us\ell\nu,*} \mathcal{O}_i^{us\ell\nu,\dagger} \,. \tag{5.6}$$

The operators $\mathcal{O}_i$ are constructed in the same way as in equations 5.4 and 5.5. From this follows that the operators $\mathcal{O}_i^\dagger$ for ℓ^- decay are

$$\begin{aligned}
\mathcal{O}_{V,L,L}^{us\ell\nu,\dagger} &= \left[\bar{s}\gamma^\mu P_L u\right]\left[\bar{\nu}\gamma_\mu P_L \ell\right], & \mathcal{O}_{V,R,L}^{us\ell\nu,\dagger} &= \left[\bar{s}\gamma^\mu P_R u\right]\left[\bar{\nu}\gamma_\mu P_L \ell\right], \\
\mathcal{O}_{S,L,L}^{us\ell\nu,\dagger} &= \left[\bar{s}P_R u\right]\left[\bar{\nu}P_R \ell\right], & \mathcal{O}_{S,R,L}^{us\ell\nu,\dagger} &= \left[\bar{s}P_L u\right]\left[\bar{\nu}P_R \ell\right], \\
\mathcal{O}_{T,L}^{us\ell\nu,\dagger} &= \left[\bar{s}\sigma^{\mu\nu} u\right]\left[\bar{\nu}\sigma_{\mu\nu} P_R \ell\right].
\end{aligned} \tag{5.7}$$

Adding the option of right-handed neutrinos again, we find

$$\begin{aligned}
\mathcal{O}_{V,L,R}^{us\ell\nu,\dagger} &= \left[\bar{s}\gamma^\mu P_L u\right]\left[\bar{\nu}\gamma_\mu P_R \ell\right], & \mathcal{O}_{V,R,R}^{us\ell\nu,\dagger} &= \left[\bar{s}\gamma^\mu P_R u\right]\left[\bar{\nu}\gamma_\mu P_R \ell\right], \\
\mathcal{O}_{S,L,R}^{us\ell\nu,\dagger} &= \left[\bar{s}P_R u\right]\left[\bar{\nu}P_L \ell\right], & \mathcal{O}_{S,R,R}^{us\ell\nu,\dagger} &= \left[\bar{s}P_L u\right]\left[\bar{\nu}P_L \ell\right], \\
\mathcal{O}_{T,R}^{us\ell\nu,\dagger} &= \left[\bar{s}\sigma^{\mu\nu} u\right]\left[\bar{\nu}\sigma_{\mu\nu} P_L \ell\right].
\end{aligned} \tag{5.8}$$

Since the B^- decay can occur in a different manner than the ℓ^- decay, the two operator sets must be used independently.

5.2 $B^- \to \pi^0$ Form Factors

Since the first part of the process is $B^- \to \pi^0 W^-$, the form factors of this process are more involved than before. The expressions for the decay constants of this process are formulated in [15]. All decay constants are functions of P^2, where P is the momentum of the W^- boson. The expression for the vector matrix element between B^- and π,

$$\langle \pi^0(p')|\, \bar{u}\gamma^\mu b\, |B^-(p)\rangle = f_+\left[(p+p')^\mu - \frac{M_B^2 - M_\pi^2}{P^2}P^\mu\right] + f_0 \frac{M_B^2 - M_\pi^2}{P^2}P^\mu, \tag{5.9}$$

can be used directly. For the scalar currents, using the Dirac equation 4.15, we derive

$$\langle \pi^0(p')|\, \bar{u}b\, |B^-(p)\rangle = f_0 \frac{M_B^2 - M_\pi^2}{m_b - m_u}. \tag{5.10}$$

The expression for the tensor current is derived using

$$M_B^2 - M_\pi^2 = (p+p')_\nu (p-p')^\nu. \tag{5.11}$$

From this we find

$$\langle \pi^0(p')|\, \bar{u}\sigma_{\mu\nu} b\, |B^-(p)\rangle = \frac{i f_T}{M_B + M_\pi}\left[P_\nu (p+p')_\mu - (p+p')_\nu P_\mu\right]. \tag{5.12}$$

For finding the matrix element, we use expressions formulated with chiral projection operators. Since the terms with γ^5 involved are zero, the expressions are independent of the projection operator.

In the case of $B^- \to \pi^0 W^-$ they are:

$$\langle \pi^0(p')| \bar{u}\gamma^\mu P_{\underset{R}{L}} b |B^-(p)\rangle = \frac{f_+}{2}(p+p')^\mu + \frac{f_0 - f_+}{2}\frac{M_B^2 - M_\pi^2}{P^2}P^\mu \,, \tag{5.13}$$

$$\langle \pi^0(p')| \bar{u}P_{\underset{R}{L}} b |B^-(p)\rangle = \frac{f_0}{2}\frac{M_B^2 - M_\pi^2}{m_b - m_u} \,, \tag{5.14}$$

$$\langle \pi^0(p')| \bar{u}\sigma_{\mu\nu} P_{\underset{R}{L}} b |B^-(p)\rangle = \frac{if_T}{2(M_B + M_\pi)}\left[P_\nu (p+p')_\mu - (p+p')_\nu P_\mu\right] . \tag{5.15}$$

The expressions involving the Kaon decay constant used are the same as in section 4. They are

$$\begin{aligned} \langle K^-(k)| \bar{s}\gamma_\mu P_{\underset{R}{L}} u |0\rangle &= \pm i\frac{f_K}{2}k_\mu \,, \\ \langle K^-(k)| \bar{s}P_{\underset{R}{L}} u |0\rangle &= \mp\frac{if_K M_K^2}{2(m_s + m_u)} \,. \end{aligned} \tag{5.16}$$

Now that we have formulated all expressions with the decay constants we need later on, we are now ready to compute the amplitude.

5.3 The Amplitude

From the two Lagrangians, amplitude for background process II is constructed in the following way

$$i\mathcal{M} = i\left(\frac{4G_F}{\sqrt{2}}\right)^2 V_{ub}V_{us}^* \sum_{i,j} \mathcal{C}_i^{us\ell\nu,*}\mathcal{C}_j^{ub\ell\nu}\mathcal{M}_{ij}\frac{i}{Q^2 - m_\ell^2 + im_\ell\Gamma_\ell} \,, \tag{5.17}$$

in which

$$\mathcal{M}_{ij} = \sum_{\ell \text{ spin}} \langle \nu(q_1)K^-(k)| \mathcal{O}_i^{us\ell\nu,\dagger} |\ell^-(Q)\rangle \langle \ell^-(Q)\bar{\nu}(q_2)\pi^0(p')| \mathcal{O}_j^{ub\ell\nu} |B^-(p)\rangle \,. \tag{5.18}$$

Let us first look at the SM case, using operators $\mathcal{O}_{V_{L,L}}^{ub\ell\nu}$ and $\mathcal{O}_{V_{L,L}}^{us\ell\nu,\dagger}$. The matrix element then becomes

$$\begin{aligned} \mathcal{M}_{V_{L,L}V_{L,L}} = \sum_{\ell \text{ spin}} &\left[\bar{u}(q_1)\gamma^\alpha P_L u(Q)\right]\left[\bar{u}(Q)\gamma^\mu P_L v(q_2)\right] \\ &\langle K^-(k)| \bar{s}\gamma_\alpha P_L u |0\rangle \langle \pi(p')| \bar{u}\gamma_\mu P_L b |B^-(p)\rangle \,. \end{aligned} \tag{5.19}$$

Using the same steps and the Dirac equation as in the previous background process, we find

$$\begin{aligned}
\mathcal{M}_{V_{L,L}V_{L,L}} &= \sum_{\ell \text{ spin}} \left[\bar{u}(q_1)\gamma^\alpha P_L u(Q)\right]\left[\bar{u}(Q)\gamma^\mu P_L v(q_2)\right] \\
&\quad \frac{if_k}{2}k_\alpha\left(\frac{f_+}{2}(p+p')_\mu + \frac{f_0-f_+}{2}\frac{M_B^2-M_\pi^2}{P^2}P_\mu\right), \\
&= \sum_{\ell \text{ spin}} \left[\bar{u}(q_1)P_R \not{Q} u(Q)\right]\left[\bar{u}(Q)\gamma^\mu P_L v(q_2)\right] \\
&\quad \frac{if_k}{4}\left(f_+(p+p')_\mu + (f_0-f_+)\frac{M_B^2-M_\pi^2}{P^2}P_\mu\right), \\
&= \left[\bar{u}(q_1)P_R(\not{Q}+m_\ell)P_R\gamma^\mu v(q_2)\right] m_\ell \\
&\quad \frac{if_k}{4}\left(f_+(p+p')_\mu + (f_0-f_+)\frac{M_B^2-M_\pi^2}{P^2}P_\mu\right), \\
&= \left[\bar{u}(q_1)P_R\gamma^\mu v(q_2)\right] m_\ell^2 \frac{if_k}{4}\left(f_+(p+p')_\mu + (f_0-f_+)\frac{M_B^2-M_\pi^2}{P^2}P_\mu\right).
\end{aligned} \tag{5.20}$$

Because the momentum related to the B^- meson decay cannot be simplified as in the previous background, it will stay in the expression for now.
The element $\mathcal{M}_{V_{L,L}V_{L,L}}$ is the SM contribution to the matrix elements $\mathcal{M}_{ij}$. Since both processes $B^- \to \pi^0 \ell^- \bar{\nu}$ and $\ell \to K^- \nu$ are mediated by ten different operators each, there are 100 elements $\mathcal{M}_{ij}$. However, some of them are zero or differ from one another only in sign. The independent elements $\mathcal{M}_{ij}$ can be found in Appendix C. From these elements, all others are found easily applying the following rules:

- The elements are independent of the chirality of the hadronic current of the decay of the B^- meson.
- Elements with an opposite chirality in the hadronic current of the kaon production are of opposite sign.
- Elements with a tensor current in the kaon production are zero, as we have seen in chapter 4.

Together, these elements add up to the full amplitude given in equation 5.17.
For our further calculation, the spinor parts S of these amplitudes are most relevant, since the square of constants is computed trivially. There are twelve different possibilities, being

$$\begin{aligned}
S_1 &= \left[\bar{u}(q_1)P_{\substack{L\\R}}v(q_2)\right], & S_{\not{Q}} &= \left[\bar{u}(q_1)P_{\substack{L\\R}}\not{Q}v(q_2)\right], \\
S_\gamma^\mu &= \left[\bar{u}(q_1)P_{\substack{L\\R}}\gamma^\mu v(q_2)\right], & S_{\not{Q}\gamma}^\mu &= \left[\bar{u}(q_1)P_{\substack{L\\R}}\not{Q}\gamma^\mu v(q_2)\right], \\
S_\sigma^{\mu\nu} &= \left[\bar{u}(q_1)P_{\substack{L\\R}}\sigma^{\mu\nu} v(q_2)\right], & S_{\not{Q}\sigma}^{\mu\nu} &= \left[\bar{u}(q_1)P_{\substack{L\\R}}\not{Q}\sigma^{\mu\nu} v(q_2)\right].
\end{aligned} \tag{5.21}$$

These spinor parts form the key element in computing the amplitude squared.

5.4 The Amplitude Squared

In the previous section all matrix elements are calculated and simplified. The twelve different spinor parts S need to be multiplied by all twelve spinor parts $S^\dagger$.
The case of the SM contains $S^\mu_{\gamma,R}$. The spinor part squared makes

$$\begin{aligned}\left\langle S^\mu_{\gamma,R} S^{\nu\dagger}_{\gamma,R}\right\rangle &= \sum_{\text{spin}} \left[\bar{u}(q_1) P_R \gamma^\mu v(q_2)\right] \left[\bar{v}(q_2)\gamma^\nu P_L u(q_1)\right] , \\ &= \text{Tr}[\not{q}_1 \gamma^\mu \not{q}_2 \gamma^\nu P_L] .\end{aligned} \tag{5.22}$$

Making use of the properties of Dirac's matrices stated in [18], this becomes

$$\left\langle S^\mu_{\gamma,R} S^{\nu\dagger}_{\gamma,R}\right\rangle = 2q_{1,\alpha} q_{2,\beta} \left(\eta^{\alpha\mu}\eta^{\beta\nu} - \eta^{\alpha\beta}\eta^{\mu\nu} + \eta^{\alpha\nu}\eta^{\beta\mu} + i\epsilon^{\alpha\mu\beta\nu}\right) . \tag{5.23}$$

So far, this is the same as in the first background process. However, the contractions with the momenta are different due to the pion in the final state. The squared amplitude at this point looks like

$$\begin{aligned}\left\langle |\mathcal{M}_{V_{L,L}V_{L,L}}|^2\right\rangle =& m_\ell^4 \frac{f_k^2}{16} \left(f_+(p+p')_\mu + (f_0 - f_+)\frac{M_B^2 - M_\pi^2}{P^2} P_\mu\right) \\ & \left(f_+(p+p')_\nu + (f_0 - f_+)\frac{M_B^2 - M_\pi^2}{P^2} P_\nu\right) \\ & 2q_{1,\alpha} q_{2,\beta} \left(\eta^{\alpha\mu}\eta^{\beta\nu} - \eta^{\alpha\beta}\eta^{\mu\nu} + \eta^{\alpha\nu}\eta^{\beta\mu} + i\epsilon^{\alpha\mu\beta\nu}\right) .\end{aligned} \tag{5.24}$$

The Levi-Civita symbol vanishes in all contractions. In two cases, it is contracted with the same momentum twice, from where it vanishes due to the antisymmetric properties of the symbol. The other two contractions cancel each other.
This leads to the SM squared amplitude being

$$\begin{aligned}\left\langle |\mathcal{M}_{V_{L,L}V_{L,L}}|^2\right\rangle \frac{8}{m_\ell^4 f_k^2} =& f_+^2 \left(2q_1\cdot(p+p')\, q_2\cdot(p+p') - q_1\cdot q_2\,(p+p')^2\right) \\ & + 2(f_0 - f_+) f_+ \frac{M_B^2 - M_\pi^2}{P^2} \left(q_1\cdot(p+p')\, q_2\cdot P + q_1\cdot P\, q_2\cdot(p+p') - q_1\cdot q_2\, P\cdot(p+p')\right) \\ & + (f_0 - f_+)^2 \left(\frac{M_B^2 - M_\pi^2}{P^2}\right)^2 \left(2q_1\cdot P\, q_2\cdot P - q_1\cdot q_2\, P^2\right) .\end{aligned} \tag{5.25}$$

In the case of the first background process, it was relatively easy to compute the required dot products. Until now everything was frame independent. However, to find the required dot products, two Lorentz boosts need to be performed since the momenta are defined in three different frames. To define the momenta, the Gottfried-Jackson frame is used explicitly. The frames and the Lorentz boosts needed are stated in Appendix A.4. For the analysis of the squared amplitudes in the SM and beyond, a lot of dot products come into play. Since the kaon momentum was contracted before, the dot products with k^α are irrelevant. All dot products not involving the kaon momentum k^α appear in at least one of the squared amplitudes.
Some of the expressions of the required dot products are lengthy, especially those where two Lorentz transformations are required. The SM squared amplitude in terms of the masses and angles therefore becomes very lengthy and not illuminating. I will therefore not give it here.

In section 5.3, 12 different spinor parts of the amplitude are given. I will not provide all 144 combinations of the spinor parts. However, a few comments are worth mentioning.
Firstly, a combination of one of S_1, $S^{\mu}_{\not{q}\gamma}$ or $S^{\mu\nu}_{\sigma}$ with the complex conjugate of one of $S_{\not{q}}$, S^{μ}_{γ} or $S^{\mu\nu}_{\not{q}\sigma}$ or vice versa will always be zero since this will give an odd number of gamma matrices, of which the trace is zero. This halves the number of terms contributing to the squared amplitude.
Secondly, all terms contain a projection operator. Since $P_L P_R = 0$, half of the remaining terms vanish. The terms that remain, always contain the same projection operator in the initial (not yet conjugated) spinor part.
These two simplifications leave us with 36 different combinations of spinor parts. The spinor parts occur twice in the different amplitudes given in Appendix C, providing every spinor part with two different sets of momenta with which to be contracted.

5.5 What's next?

The expressions become more and more lengthy. Until this point, it has still been possible to carry out this analysis analytically. At this point, however, we stumble into two problems that make it inconvenient to go on analytically.
The first problem is the dot product of the momenta. Since two Lorentz transformations have to be performed for some dot products, the expressions become very lengthy.
The second problem has to do with the lost momentum. We aim for $\frac{d\mathcal{B}}{dq^2_{lost}}(q^2_{lost})$, where q^2_{lost} contains not only the momentum of the two neutrinos, but also that of the missed pion. We define

$$q^2_{lost} = (q_1 + q_2 + p')^2 \,. \tag{5.26}$$

This expression does not appear in the squared amplitude in this or another convenient form. Taken together, these problems lead to the conclusion that the rest of the calculations must be carried out with a computer program.
It is beyond the scope of this project to complete this analysis. To complete the analysis, a few more steps are necessary. To begin with, a full squared amplitude needs to be calculated numerically. The q^2_{lost} needs to be dragged out of this expression. In Appendix A.4 a start is made on the phase space element. This needs to be completed and the phase space integration needs to be performed. The branching ratio is then found using equation 5.2.

Chapter 6

Conclusion

The goal of this research was to analytically calculate lepton mediated $B^- \to K^- \nu\bar{\nu}$ processes that are a background to the loop-induced process $B^- \to K^- \nu\bar{\nu}$, including effects of new physics, making use of the Weak Effective Theory. The results make it possible to interpret the measurement of $B^- \to K^- \nu\bar{\nu}$ in terms of models beyond the Standard Model. In light of this, two processes were studied: the irreducible background process $B^- \to \ell^- [\to K^- \nu]\bar{\nu}$, and the reducible background process $B^- \to \pi^0 \ell^- [\to K^- \nu]\bar{\nu}$. The latter is a reducible background process to the loop-induced $B^- \to K^- \nu\bar{\nu}$ since the pion π^0 is charge neutral and long-lived, and can therefore be easily missed in a detector.

The analysis of background process I, mediated by a τ^- lepton $B^- \to \tau^- [\to K^- \nu]\bar{\nu}$ considered four different cases. When considering only nonzero Wilson coefficients for operators with left-handed leptonic current, the branching ratio would decrease linearly as a function of q^2, approaching zero as q^2 reaches its upper bound. The obtained differential branching ratios have the same shape, and differ only in their slope.
While looking at nonzero Wilson coefficients for operators with right-handed leptonic current only, the same shape appears. However, when allowing Wilson coefficients with right-handed and left-handed leptonic current to be nonzero at the same time, an extra term appears. This causes the shape of the branching ratio to change. When choosing the Wilson coefficients such that the contribution with right-handed leptonic current is equal to the contribution with left-handed leptonic current, one finds a branching ratio that is independent of q^2. The shape of the normalized branching ratio is then a horizontal line. Changing the relative magnitude of the Wilson coefficients makes all shapes between these two lines possible.
Due to this change in shape, the analysis of the Belle II collaboration could be miss important features – if there were new physics in this background process. In order to take the new physics in this background process properly into account, the Belle II collaboration should redo a part of their analysis.
Apart from the shape of the differential branching ratio, the values are plotted of the Wilson coefficients for which the same branching ratio would be found. These plots show that a small change in the Wilson coefficients could lead to a big difference in the branching ratio; they also show which change in the Wilson coefficients would increase in the branching ratio. Furthermore,

these plots show degeneracies. To resolve these, the shape analysis is needed.
Since both the initial state and the final state of the loop-induced signal process and the lepton mediated background process 1 are identical, the amplitudes need to be summed coherently. However, the interference term arising from this scales with an extra factor of G_F and is therefore negligible.

While analyzing the reducible background process $B^- \to \pi^0\tau[\to K^-\nu]\bar{\nu}$ we stumbled into several problems. Unlike the first background process, where a lot of amplitudes were similar to one another or zero, here many different amplitudes were encountered. This led to even more terms in the squared amplitude. Furthermore, in the first background process, only one Lorentz boost was needed, but in the second background process, two Lorentz boosts were needed. This made the expressions messier. Lastly, it was more difficult to get the q^2_{lost} out of the expression.
Although much of the analysis could be carried out analytically, the rest of the analysis should be carried out numerically. This was, however, beyond the scope of this project. In order to take new physics effects of the background process $B^- \to \pi^0\tau[\to K^-\nu]\bar{\nu}$ into account, the numerical part of analysis must be completed. This requires finding the dependence on q^2_{lost} and carrying out the integration over the phase space element.

Bibliography

[1] HPQCD collaboration, *Standard Model predictions for $B \to K\ell^+\ell^-$, $B \to K\ell_1^-\ell_2^+$ and $B \to K\nu\bar{\nu}$ using form factors from $N_f = 2+1+1$ lattice QCD*, *Phys. Rev. D* **107** (2023) 014511 [2207.13371].

[2] Belle-II collaboration, *Evidence for $B^+ \to K^+\nu\bar{\nu}$ decays*, *Phys. Rev. D* **109** (2024) 112006 [2311.14647].

[3] L. Allwicher, D. Becirevic, G. Piazza, S. Rosauro-Alcaraz and O. Sumensari, *Understanding the first measurement of $\mathcal{B}(B \to K\nu\bar{\nu})$*, *Phys. Lett. B* **848** (2024) 138411 [2309.02246].

[4] R. Bause, H. Gisbert and G. Hiller, *Implications of an enhanced $B \to K\nu\bar{\nu}$ branching ratio*, *Phys. Rev. D* **109** (2024) 015006 [2309.00075].

[5] J. Martin Camalich, M. Pospelov, P.N.H. Vuong, R. Ziegler and J. Zupan, *Quark Flavor Phenomenology of the QCD Axion*, *Phys. Rev. D* **102** (2020) 015023 [2002.04623].

[6] T. Ferber, A. Filimonova, R. Schäfer and S. Westhoff, *Displaced or invisible? ALPs from B decays at Belle II*, *JHEP* **04** (2023) 131 [2201.06580].

[7] A. Filimonova, R. Schäfer and S. Westhoff, *Probing dark sectors with long-lived particles at BELLE II*, *Phys. Rev. D* **101** (2020) 095006 [1911.03490].

[8] W. Altmannshofer, A.J. Buras, D.M. Straub and M. Wick, *New strategies for New Physics search in $B \to K^*\nu\bar{\nu}$, $B \to K\nu\bar{\nu}$ and $B \to X_s\nu\bar{\nu}$ decays*, *JHEP* **04** (2009) 022 [0902.0160].

[9] J.F. Kamenik and C. Smith, *Tree-level contributions to the rare decays $B^+ \to \pi^+\nu\bar{\nu}$, $B^+ \to K^+\nu\bar{\nu}$, and $B^+ \to K^{*+}\nu\bar{\nu}$ in the Standard Model*, *Phys. Lett. B* **680** (2009) 471 [0908.1174].

[10] A.J. Buras, J. Girrbach-Noe, C. Niehoff and D.M. Straub, *$B \to K^{(*)}\nu\bar{\nu}$ decays in the Standard Model and beyond*, *JHEP* **02** (2015) 184 [1409.4557].

[11] Particle Data Group collaboration, *Review of Particle Physics*, *PTEP* **2022** (2022) 083C01.

[12] S.L. Glashow, J. Iliopoulos and L. Maiani, *Weak Interactions with Lepton-Hadron Symmetry*, *Phys. Rev. D* **2** (1970) 1285.

[13] Y. Grossman, *Introduction to flavor physics*, in *2009 European School of High-Energy Physics*, pp. 111–144, 2010, DOI [1006.3534].

[14] A.V. Manohar, *Introduction to Effective Field Theories*, 1804.05863.

[15] D. Leljak, B. Melić and D. van Dyk, *The $\bar{B} \to \pi$ form factors from QCD and their impact on $|V_{ub}|$*, *JHEP* **07** (2021) 036 [2102.07233].

[16] A.J. Buras, *Weak Hamiltonian, CP violation and rare decays*, in *Les Houches Summer School in Theoretical Physics, Session 68: Probing the Standard Model of Particle Interactions*, pp. 281–539, 6, 1998 [hep-ph/9806471].

[17] M. Neubert, *Effective field theory and heavy quark physics*, in *Theoretical Advanced Study Institute in Elementary Particle Physics: Physics in D $\geqq$ 4*, pp. 149–194, 12, 2005, DOI [hep-ph/0512222].

[18] M.E. Peskin and D.V. Schroeder, *An Introduction to quantum field theory*, Addison-Wesley, Reading, USA (1995), 10.1201/9780429503559.

Appendix A

Kinematics and Phase Space Elements

In our calculations of the differential decay widths of the signal process and the background processes, we use the common convention for the notation and normalization of the n-body Lorentz invariant phase space elements. Then

$$d\Phi_n(P; p_1, ..., p_n) = \delta^4\left(P - \sum_{i=1}^{n} p_i\right) \prod_{i=1}^{n} \frac{d^3 p_i}{(2\pi)^3 2E_i}. \tag{A.1}$$

We further use the following recursion formula to factorize the N-body phase space element into a sequence of two-body phase space elements:

$$d\Phi_n(P; p_1, ..., p_n) = d\Phi_j(q; p_1, ..., p_j)\, d\Phi_{n-j+1}(P; q, p_{j+1}, ..., p_n)(2\pi)^3 dq^2\,. \tag{A.2}$$

The remainder of this appendix is dedicated to the definition of the nested two-body reference frames in the Gottfried-Jackson convention (appendix A.1), the details of the kinematics for the signal process (appendix A.2), and the two background processes (appendix A.3 and appendix A.4). Though the signal process is not described in detail in this thesis, the definitions of the momenta of the background processes are defined parallel to the signal process. Therefore the signal process is included in this appendix on kinematics.

A.1 Gottfried-Jackson Frame

The Gottfried-Jackson convention is used to construct the reference frame of a particle produced in a two-body decay process. Let this two-body process be $a \to bc$, with $\vec{p}_b^{\,a}$ and $\vec{p}_c^{\,a}$ denoting the three-momenta of the particles b and c in the a center-of-mass frame. Then the coordinate system of the b center-of-mass frame, used to specify the kinematics of a secondary decay of b, is defined as

$$\hat{z}^b = \frac{\vec{p}_b^{\,a}}{|\vec{p}_b^{\,a}|}\,, \quad \hat{y}^b = \frac{\hat{z}^a \times \hat{z}^b}{|\hat{z}^a \times \hat{z}^b|}\,, \quad \hat{x}^b = \frac{\hat{y}^b \times \hat{z}^b}{|\hat{y}^b \times \hat{z}^b|}\,. \tag{A.3}$$

Using this convention, we define the helicity angle θ_{ba} and the azimuthal angle ϕ_{ba} associated with the particle b in the center-of-mass frame of particle a

$$\begin{aligned} \cos\theta_{ba} &\equiv \frac{\vec{p}_b^{\,a} \cdot \hat{z}^a}{|\vec{p}_b^{\,a}|} \\ \cos\phi_{ba} &\equiv \frac{\vec{p}_b^{\,a} \cdot \hat{x}^a}{|\vec{p}_b^{\,a}|\,|\sin\theta_{ba}|} \end{aligned} \tag{A.4}$$

A.2 Signal Process: $B^- \to K^-\nu\bar{\nu}$

We use the following convention to label the kinematics of the signal process,

$$B^-(p) \to K^-(k)\nu(q_1)\bar{\nu}(q_2)\,. \tag{A.5}$$

We chose to express its three-body phase space element as a cascade of two two-body phase space elements, corresponding to

$$B^-(p) \to K^-(k)X(q)[\to \nu(q_1)\bar{\nu}(q_2)], \tag{A.6}$$

where the "mediator" X is only used to simplify the phase-space calculation. Since the initial B meson is a pseudoscalar state, the decay is isotropic and we can choose the momenta in the B center-of-mass system (c.m.s.):

$$\begin{aligned} p^\mu\big|_{B\text{-c.m.s.}} &= (M_B, 0, 0, 0)^T\,, \\ k^\mu\big|_{B\text{-c.m.s.}} &= (E_K, 0, 0, -|\vec{q}|)^T\,, \\ q^\mu\big|_{B\text{-c.m.s.}} &= (E_q, 0, 0, +|\vec{q}|)^T\,. \end{aligned} \tag{A.7}$$

Here we abbreviate

$$\begin{aligned} |\vec{q}| &= \frac{\sqrt{\lambda(M_B^2, M_K^2, q^2)}}{2M_B}\,, \\ E_K^2 = M_K^2 + |\vec{q}|^2 &= \left[\frac{M_B^2 + M_K^2 - q^2}{2M_B}\right]^2\,, \quad E_q^2 = q^2 + |\vec{q}|^2 = \left[\frac{M_B^2 - M_K^2 + q^2}{2M_B}\right]^2\,, \end{aligned} \tag{A.8}$$

where $\lambda(a,b,c) = a^2 + b^2 + c^2 - 2ab - 2ac - 2bc$ is the Källen function. We construct the momenta in the c.m.s. of the "mediator" X, using the Gottfried-Jackson convention; see appendix A.1:

$$\begin{aligned} q^\mu\big|_{X\text{-c.m.s.}} &= (\sqrt{q^2}, 0, 0, 0)\,, \\ q_1^\mu\big|_{X\text{-c.m.s.}} &= (|E_{\nu X}|, +|E_{\nu X}|\cos\phi_{\nu X}\sin\theta_{\nu X}, +|E_{\nu X}|\sin\phi_{\nu X}\sin\theta_{\nu X}, +|E_{\nu X}|\cos\theta_{\nu X})\,, \\ q_2^\mu\big|_{X\text{-c.m.s.}} &= (|E_{\nu X}|, -|E_{\nu X}|\cos\phi_{\nu X}\sin\theta_{\nu X}, -|E_{\nu X}|\sin\phi_{\nu X}\sin\theta_{\nu X}, -|E_{\nu X}|\cos\theta_{\nu X})\,. \end{aligned} \tag{A.9}$$

Here $E_\nu = \sqrt{q^2}/2$. The Lorentz boost along the z axis to transform a four vector in the B-c.m.s. into a four vector in the X-c.m.s. is given by

$$\Lambda^\mu{}_\nu = \begin{pmatrix} \gamma & 0 & 0 & \beta\gamma \\ 0 & 1 & 0 & 0 \\ 0 & 0 & 1 & 0 \\ \beta\gamma & 0 & 0 & \gamma \end{pmatrix} \tag{A.10}$$

with

$$q^\mu\big|_{X\text{-c.m.s.}} = \Lambda^\mu_\nu q^\mu\big|_{B\text{-c.m.s.}}\,, \tag{A.11}$$

$$(\sqrt{q^2},0,0,0)^T = (\gamma\left[E_q + \beta|\vec{q}|\right]\big|_{B\text{-c.m.s.}}, 0, 0, \gamma\left[\beta E_q + |\vec{q}|\right]\big|_{B\text{-c.m.s.}})^T\,. \tag{A.12}$$

This leads to

$$\begin{aligned} \beta &= -\frac{|\vec{q}|}{E_q}\Big|_{B\text{-c.m.s.}} \\ \gamma &= E_q\big|_{B\text{-c.m.s.}}/\sqrt{q^2}\,. \end{aligned} \tag{A.13}$$

In the signal process, the momentum that is missed in the detector is easily constructed due to momentum conservation. The lost momentum is

$$(q_1+q_2)^2 = q^2\,. \tag{A.14}$$

We identify two Lorentz invariant quantities that we will use to describe our phase space elements. They are

$$\begin{aligned} &(q_1+q_2)^2 = q^2 \\ &k\cdot(q_2-q_1) = M_B|\vec{q}|\big|_{B\text{-c.m.s.}}\cos\theta\big|_{X\text{-c.m.s.}} = \frac{\sqrt{\lambda(M_B^2,M_K^2,q^2)}}{2}\cos\theta\big|_{X\text{-c.m.s.}}\,. \end{aligned} \tag{A.15}$$

The two-body phase space element for the decay $B^-(p)\to K^-(k)X(q)$ reads

$$\begin{aligned} d\Phi_2(p;k,q) &= \delta^4(p-k-q)\frac{d^3q}{(2\pi)^3 2E_q}\frac{d^3k}{(2\pi)^3 2E_k} \\ &= \delta^4(p-k-q)\frac{d^3q}{(2\pi)^3 2E_q}\frac{d^4k}{(2\pi)^3}\delta(k^2-M_K^2)\Theta(E_k) \\ &= \frac{1}{(2\pi)^6}\frac{d^3q}{2E_q}\delta(M_B^2+q^2-M_K^2-2M_BE_q)\Theta(E_k)\,, \\ &= \frac{1}{(2\pi)^5}\frac{M_B^2-q^2}{4M_B^2}\Theta(E_k) \end{aligned} \tag{A.16}$$

The two-body phase space element for the decay $X(q)\to\nu(q_1)\bar{\nu}(q_2)$ reads

$$d\Phi_2(q;q_1,q_2) = \frac{1}{(2\pi)^6}\frac{d^3q_1}{2E_\nu}\delta\left(q^2-2\sqrt{q^2}|E_{\nu X|}\right)\Theta(E_\nu) \quad = \frac{d\cos\theta}{8(2\pi)^5}\Theta(E_\nu) \tag{A.17}$$

We can trivially execute the integration over $\phi_{\nu X}$ since the decay's matrix element does not depend on it.[1] Using the recursion formula eq. (A.2), we arrive at the full three-body phase space element

$$d\Phi_3(p;k,q_1,q_2) = d\Phi_2(p;k,q)\, d\Phi_2(q;q_1,q_2)(2\pi)^3 dq^2 \tag{A.18}$$

$$= \frac{d\cos\theta dq^2}{8(2\pi)^7} \frac{M_B^2 - q^2}{4M_B^2} \Theta(E_k)\Theta(E_\nu) \tag{A.19}$$

A.3 Background Process I: $B^- \to \tau^-(\to K^-\nu)\bar{\nu}$

We use the following convention to label the kinematics of the first background process considered in this work,

$$B^-(p) \to \tau^-(Q)\left[\to K^-(k)\nu(q_1)\right]\bar{\nu}(q_2)\,. \tag{A.20}$$

Naturally, this implies that $Q^\mu \equiv k^\mu + q_1^\mu$. Since the initial B meson is a pseudoscalar state, the decay is isotropic and we can choose the momenta in the B center-of-mass system (c.m.s.):

$$\begin{aligned} p^\mu\big|_{B\text{-c.m.s.}} &= (M_B, 0, 0, 0)\,, \qquad Q^\mu\big|_{B\text{-c.m.s.}} = (E_Q, 0, 0, +|\vec{Q}|)\,, \\ q_2^\mu\big|_{B\text{-c.m.s.}} &= (|\vec{Q}|, 0, 0, -|\vec{Q}|)\,. \end{aligned} \tag{A.21}$$

Here, we abbreviate

$$|\vec{Q}| = \frac{\sqrt{\lambda(M_B^2, Q^2, 0)}}{2M_B} = \frac{M_B^2 - Q^2}{2M_B}\,, \quad E_Q^2 = Q^2 + |\vec{Q}|^2 = \left[\frac{M_B^2 + Q^2}{2M_B}\right]^2\,. \tag{A.22}$$

where $\lambda(a,b,c) = a^2 + b^2 + c^2 - 2ab - 2ac - 2bc$ is the Källen function. We construct the c.m.s. of the secondary decay $\tau^-(Q) \to K^-(k)\nu(q_1)$ using the Gottfried-Jackson convention

$$\begin{aligned} Q^\mu\big|_{\tau\text{-c.m.s.}} &= (\sqrt{Q^2}, 0, 0, 0)\,, \\ k^\mu\big|_{\tau\text{-c.m.s.}} &= (E_K, |\vec{k}|\cos\phi\sin\theta, |\vec{k}|\sin\phi\sin\theta, |\vec{k}|\cos\theta)\,, \\ q_1^\mu\big|_{\tau\text{-c.m.s.}} &= (|\vec{k}|, -|\vec{k}|\cos\phi\sin\theta, -|\vec{k}|\sin\phi\sin\theta, -|\vec{k}|\cos\theta)\,. \end{aligned} \tag{A.23}$$

The kaon and the neutrino momenta are on-shell, and hence $k^2 = M_K^2$ and $q_1^2 = 0$. In the above, we abbreviate

$$|\vec{k}| = \frac{\sqrt{\lambda(Q^2, M_K^2, 0)}}{2\sqrt{Q^2}} = \frac{Q^2 - M_K^2}{2\sqrt{Q^2}}\,, \quad E_K^2 = M_K^2 + |\vec{k}|^2 = \left[\frac{Q^2 + M_K^2}{2\sqrt{Q^2}}\right]^2\,. \tag{A.24}$$

The Lorentz boost reads as in equation A.10, with

$$\begin{aligned} \beta &= -\frac{|\vec{Q}|}{E_Q} \\ \gamma &= \frac{E_Q}{\sqrt{Q^2}}\,. \end{aligned} \tag{A.25}$$

[1] This is because no scalar product of any of the four-vectors p, k, q_1 and q_2 depends on $\phi_{\nu X}$, and no Levi-Civita symbol can be constructed from these four-vectors since they are linearly dependent.

The momentum that is missed in the detector is that of the two neutrinos. We define

$$\begin{aligned} q^2 &= (q_1 + q_2)^2 \\ &= 0 + 2q_1 \cdot q_2 + 0\,. \end{aligned} \tag{A.26}$$

Using a Lorentz boost on q_1^μ to express it in the B^- c.m.s we find

$$q_1^\mu\big|_{B\text{-c.m.s.}} = \left(E_Q - |\vec{Q}|\cos\theta, -m_\tau \cos\phi \sin\theta, -m_\tau \sin\phi \sin\theta, |\vec{Q}| - E_Q \cos\theta\right) \frac{|\vec{k}|}{m_\tau}\,. \tag{A.27}$$

Therefore the lost momentum is

$$\begin{aligned} q^2 &= 2\frac{|\vec{Q}||\vec{k}|}{m_\tau}(1-\cos\theta)(E + |\vec{Q}|) \\ &= 2\frac{|\vec{Q}||\vec{k}|M_B}{m_\tau}(1-\cos\theta). \end{aligned} \tag{A.28}$$

We identify two Lorentz invariant quantities that we will use to describe our phase space elements with. They are

$$\begin{aligned} (k+q_1)^2 &= Q^2 \\ q_2\cdot(k-q_1) &= \frac{|\vec{Q}|M_B}{\sqrt{Q^2}}\left(E_k - |\vec{k}| - 2|\vec{k}|\cos\theta\right)\big|_{Q\text{-c.m.s.}}\,. \end{aligned} \tag{A.29}$$

The two-body phase space element for the decay $B^-(p) \to \tau(Q)\bar{\nu}(q_2)$ reads

$$\begin{aligned} d\Phi_2(p;Q,q_2) &= \delta^4(p-Q-q_2)\frac{d^3Q}{(2\pi)^3 2E_\tau}\frac{d^3q_2}{(2\pi)^3 2E_{\bar{\nu}}} \\ &= \frac{1}{(2\pi)^5}\frac{M_B^2 - Q^2}{4M_B^2}\theta(M_B - E_\tau)\,. \end{aligned} \tag{A.30}$$

The two-body phase space element for the decay $\tau(Q) \to K^-(k)\nu(q_1)$ reads

$$\begin{aligned} d\Phi_2(Q;k,q_1) &= \delta^4(Q-k-q_1)\frac{d^3k}{(2\pi)^3 2E_K}\frac{d^3q_1}{(2\pi)^3 2E_\nu} \\ &= \frac{1}{(2\pi)^6}\, d\cos\theta d\phi\, \frac{(Q^2 - M_K^2)}{8Q^2}\theta(m_\tau - E_K)\,. \end{aligned} \tag{A.31}$$

Footnote 1 applies also here, with obvious replacements. Using the recursion formula eq. (A.2), we arrive at the full three-body phase space element

$$d\Phi_3(p;k,q_1,q_2) = d\Phi_2(p;Q,q_2)\, d\Phi_2(Q;k,q_1)(2\pi)^3 dQ^2 \tag{A.32}$$

$$= \frac{d\cos\theta\, dQ^2}{32(2\pi)^7}\,\frac{Q^2 - M_K^2}{Q^2}\,\frac{M_B^2 - Q^2}{M_B^2}\,\theta(M_B - E_\tau)\,\theta(m_\tau - E_K)\,. \tag{A.33}$$

A.4 Background Process II: $B^- \to \pi^0 \ell^- (\to K^- \nu) \bar{\nu}$

We use the following convention to label the kinematics of the second background process considered in this work,

$$B^-(p) \to W(P) \left[\to \ell^-(Q) \left[\to K^-(k)\nu(q_1)\right] \bar{\nu}(q_2)\right] \pi(p') \,. \tag{A.34}$$

Naturally, this implies that $Q^\mu \equiv k^\mu + q_1^\mu$ and $P^\mu \equiv Q^\mu + q_2^\mu$. Since the initial B^- meson is a pseudoscalar state, the decay is isotropic and we can choose the momenta in the B^- center-of-mass system (c.m.s.):

$$\begin{aligned} p^\mu\big|_{B\text{-c.m.s.}} &= (M_B, 0, 0, 0) \,, & P^\mu\big|_{B\text{-c.m.s.}} &= (E_{WB}, 0, 0, +|\vec{P}_{WB}|) \,, \\ p'^\mu\big|_{B\text{-c.m.s.}} &= (E_{\pi B}, 0, 0, -|\vec{P}_{WB}|) \,. \end{aligned} \tag{A.35}$$

Here, we abbreviate

$$|\vec{P}_{WB}|^2 = \left[\frac{P_{WB}^2 + M_B^2 + M_\pi^2}{2M_B}\right]^2 - P_{WB}^2 \,, \quad E_{WB}^2 = P_{WB}^2 + |\vec{P}_{WB}|^2 = \left[\frac{P_{WB}^2 + M_B^2 + M_\pi^2}{2M_B}\right]^2 . \tag{A.36}$$

We construct the c.m.s. of the secondary decay $W^-(P) \to \ell^-(Q)^- \bar{\nu}(q_2)$ using the Gottfried-Jackson convention

$$\begin{aligned} P^\mu\big|_{W\text{-c.m.s.}} &= (\sqrt{P^2}, 0, 0, 0) \,, \\ Q^\mu\big|_{W\text{-c.m.s.}} &= (E_{\ell W}, |\vec{Q}|_{\ell W} \cos\phi_{\ell W} \sin\theta_{\ell W}, |\vec{Q}|_{\ell W} \sin\phi_{\ell W} \sin\theta_{\ell W}, |\vec{Q}|_{\ell W} \cos\theta_{\ell W}) \,, \\ q_2^\mu\big|_{W\text{-c.m.s.}} &= (|\vec{Q}|_{\ell W}, -|\vec{Q}|_{\ell W} \cos\phi_{\ell W} \sin\theta_{\ell W}, -|\vec{Q}|_{\ell W} \sin\phi_{\ell W} \sin\theta_{\ell W}, -|\vec{Q}|_{\ell W} \cos\theta_{\ell W}) \,. \end{aligned} \tag{A.37}$$

The kaon and the neutrino momenta are on-shell, and hence $k^2 = M_K^2$ and $q_1^2 = 0$. In the above, we abbreviate

$$|\vec{Q}| = \frac{P^2 - Q^2}{2\sqrt{P^2}} \,, \quad E_{\ell W}^2 = Q^2 + |\vec{Q}|^2 = \left[\frac{P^2 + Q^2}{2\sqrt{P^2}}\right]^2 . \tag{A.38}$$

The Lorentz boost reads as in equation A.10, with

$$\begin{aligned} \beta &= -\frac{|\vec{P}_{WB}|}{E_{WB}} \\ \gamma &= \frac{E_{WB}}{\sqrt{P^2}} \,. \end{aligned} \tag{A.39}$$

We construct the c.m.s. of the third decay $\ell(Q)^- \to K(k)\nu(q_1)$ using the Gottfried-Jackson convention

$$
\begin{aligned}
Q^\mu\big|_{\ell\text{-c.m.s.}} =&(m_\ell, 0, 0, 0)\,,\\
k^\mu\big|_{\ell\text{-c.m.s.}} =&(E_{k\ell},\\
&-|\vec{k}|(\cos\theta_{k\ell}\cos\phi_{\ell W}\sin\theta_{\ell W} + \frac{\sin\theta_{\ell W}}{|\sin\theta_{\ell W}|}\sin\theta_{k\ell}(\cos\theta_{\ell W}\cos\phi_{k\ell}\cos\phi_{\ell W} - \sin\phi_{k\ell}\sin\phi_{\ell W})),\\
&-|\vec{k}|(\cos\theta_{k\ell}\sin\theta_{\ell W}\sin\phi_{\ell W} + \frac{\sin\theta_{\ell W}}{|\sin\theta_{\ell W}|}\sin\theta_{k\ell}(\cos\phi_{\ell W}\sin\phi_{k\ell} + \cos\theta_{\ell W}\cos\phi_{k\ell}\sin\phi_{\ell W})),\\
&-|\vec{k}|(\cos\theta_{k\ell}\cos\theta_{\ell W} - \frac{\sin^2\theta_{\ell W}}{|\sin\theta_{\ell W}|}\cos\phi_{k\ell}\sin\theta_{k\ell}))\,,\\
q_1^\mu\big|_{\ell\text{-c.m.s.}} =&(|\vec{k}|,\\
&|\vec{k}|(\cos\theta_{k\ell}\cos\phi_{\ell W}\sin\theta_{\ell W} + \frac{\sin\theta_{\ell W}}{|\sin\theta_{\ell W}|}\sin\theta_{k\ell}(\cos\theta_{\ell W}\cos\phi_{k\ell}\cos\phi_{\ell W} - \sin\phi_{k\ell}\sin\phi_{\ell W})),\\
&|\vec{k}|(\cos\theta_{k\ell}\sin\theta_{\ell W}\sin\phi_{\ell W} + \frac{\sin\theta_{\ell W}}{|\sin\theta_{\ell W}|}\sin\theta_{k\ell}(\cos\phi_{\ell W}\sin\phi_{k\ell} + \cos\theta_{\ell W}\cos\phi_{k\ell}\sin\phi_{\ell W})),\\
&|\vec{k}|(\cos\theta_{k\ell}\cos\theta_{\ell W} - \frac{\sin^2\theta_{\ell W}}{|\sin\theta_{\ell W}|}\cos\phi_{k\ell}\sin\theta_{k\ell}))\,.
\end{aligned}
\tag{A.40}
$$

The kaon and the neutrino momenta are on-shell, and hence $k^2 = M_K^2$ and $q_1^2 = 0$. In the above, we abbreviate

$$
|\vec{k}| = \frac{Q^2 - M_K^2}{2\sqrt{Q^2}}\,, \quad E_K^2 = k^2 + |\vec{k}|^2 = \left[\frac{Q^2 + M_K^2}{2\sqrt{Q^2}}\right]^2\,. \tag{A.41}
$$

The Lorentz transformation now consists of two rotations and one boost. To transform a four-vector in the W center of mass frame to the ℓ^- center of mass frame, furthermore, two rotations are needed

$$
Q^\mu\big|_{\ell\text{-c.m.s.}} = \Lambda^\mu_\nu\, R_{-y}(\theta_{\ell W})^\nu_\beta\, R_z(\phi_{\ell W})^\beta_\alpha\, Q^\mu\big|^\alpha_{W\text{-c.m.s.}}, \tag{A.42}
$$

where the boost reads as in equation A.10, with

$$
\begin{aligned}
\beta =& -\frac{|\vec{Q}_{\ell W}|}{E_{\ell W}}\\
\gamma =& \frac{E_{\ell W}}{\sqrt{Q^2}}\,.
\end{aligned}
\tag{A.43}
$$

The momentum that is missed in the detector is that of the pion and the two neutrinos. We define

$$
q^2_{lost} = (q_1 + q_2 + p')^2\,. \tag{A.44}
$$

We identify five Lorentz invariant quantities that we will use to describe our phase space elements with. They are

$$\begin{aligned}
(k+q_1)^2 &= Q^2 \\
(Q+q_2)^2 &= P^2 \\
p'\cdot(Q-q_2) &= \frac{(|\vec{P}|^2 - E_{WB}E_{\pi B})(|\vec{Q}| - E_{\ell W}) - 2|\vec{P}||\vec{Q}|(E_{WB}-E_{\pi B})\cos\theta_{\ell W}}{\sqrt{P^2}} \\
q_2\cdot(k-q_1) &= \text{function of } \cos\theta_{K\ell} \\
\varepsilon(k,q_1,q_2,p') &= \text{function of linear combination of } \phi_{K\ell},\, \phi_{\ell W}\,.
\end{aligned} \tag{A.45}$$

The latter two functions are lengthy expressions, therefore we do not give them here.
The two-body phase space element for the decay $B^-(p) \to W^-(P)\pi(p')$ reads

$$d\Phi_2(p;P,p') = \delta^4(p-P-p')\frac{d^3P}{(2\pi)^3 2E_{WB}}\frac{d^3p'}{(2\pi)^3 2E_{\pi B}}\,. \tag{A.46}$$

The two-body phase space element for the decay $W^-(P) \to \ell^-(Q)\bar{\nu}(q_2)$ reads

$$d\Phi_2(P;Q,q_2) = \delta^4(P-Q-q_2)\frac{d^3Q}{(2\pi)^3 2E_{\ell w}}\frac{d^3q_2}{(2\pi)^3 2E_{\nu W}}\,. \tag{A.47}$$

The two-body phase space element for the decay $\ell^-(Q) \to K^-(k)\nu(q_1)$ reads

$$d\Phi_2(Q;k,q_1) = \delta^4(Q-k-q_1)\frac{d^3k}{(2\pi)^3 2E_{K\ell}}\frac{d^3q_1}{(2\pi)^3 2E_{\nu\ell}}\,. \tag{A.48}$$

The Footnote 1 regarding the Levi-Civita symbol is not applicable in this process.

Using the recursion formula eq. (A.2), we arrive at the full three-body phase space element

$$d\Phi_4(P;p',k,q_1,q_2) = d\Phi_2(p;Q,q_2)\,d\Phi_2(Q;k,q_1)(2\pi)^3 dQ^2\,. \tag{A.49}$$

Appendix B

Interference Term

Schematically, the process $B^- \to K^- \nu\bar{\nu}$ is described by two subprocesses: the "short-distance" (loop-induced) signal process with amplitude $\mathcal{M}_S$; and the "long-distance" (tree-level-induced) background process with amplitude $\mathcal{M}_{BPI}$. Since both the initial state and the final states of both processes are identical, we have to sum their amplitudes coherently. The narrow width approximation is used to get:

$$\frac{d\mathcal{B}}{dq^2} \propto \left|\mathcal{M}_S(q^2) + \mathcal{M}_{BPI}(Q^2, q^2)\right|^2 \tag{B.1}$$

$$= \left|\mathcal{M}_S(q^2)\right|^2 + 2\,\mathrm{Re}\left\{\mathcal{M}_S^*(q^2)\mathcal{M}_{BPI}(Q^2, q^2)\right\} + \left|\mathcal{M}_{BPI}(Q^2, q^2)\right|^2 \tag{B.2}$$

$$= \left|\mathcal{M}_S(q^2)\right|^2 + 2\,\mathrm{Re}\left\{\mathcal{M}_S^*(q^2)\tilde{\mathcal{M}}_B(Q^2, q^2)\frac{i}{(Q^2 - m_\tau^2) + im_\tau\Gamma_\tau}\right\} \tag{B.3}$$

$$+ \left|\tilde{\mathcal{M}}_B(Q^2, q^2)\frac{i}{(Q^2 - m_\tau^2) + im_\tau\Gamma_\tau}\right|^2 \tag{B.4}$$

$$= \left|\mathcal{M}_S(q^2)\right|^2 + 2\,\mathrm{Re}\left\{\mathcal{M}_S^*(q^2)\tilde{\mathcal{M}}_B(Q^2, q^2)\frac{i(Q^2 - m_\tau^2) + m_\tau\Gamma_\tau}{(Q^2 - m_\tau^2)^2 + m_\tau^2\Gamma_\tau^2}\right\} \tag{B.5}$$

$$+ \left|\tilde{\mathcal{M}}_B(Q^2, q^2)\right|^2 \frac{1}{(Q^2 - m_\tau^2)^2 + m_\tau^2\Gamma_\tau^2} \tag{B.6}$$

$$= \left|\mathcal{M}_S(q^2)\right|^2 + 2\,\mathrm{Re}\left\{\mathcal{M}_S^*(q^2)\tilde{\mathcal{M}}_B(Q^2, q^2)(i(Q^2 - m_\tau^2) + m_\tau\Gamma_\tau)\right\}\frac{\pi}{m_\tau\Gamma_\tau}\delta(Q^2 - m_\tau^2) \tag{B.7}$$

$$+ \left|\tilde{\mathcal{M}}_B(Q^2, q^2)\right|^2 \frac{\pi}{m_\tau\Gamma_\tau}\delta(Q^2 - m_\tau^2) \tag{B.8}$$

$$= \left|\mathcal{M}_S(q^2)\right|^2 + 2\,\mathrm{Re}\left\{\mathcal{M}_S^*(q^2)\tilde{\mathcal{M}}_B(Q^2, q^2)\right\}\pi\delta(Q^2 - m_\tau^2) + \left|\tilde{\mathcal{M}}_B(Q^2, q^2)\right|^2 \frac{\pi}{m_\tau\Gamma_\tau}\delta(Q^2 - m_\tau^2) \tag{B.9}$$

We want to know which of these terms contribute significantly. The first term scales with G_F^2. The last term scales with $\frac{G_F^4}{G_F^2} = G_F^2$. The second term, however, scales with G_F^3. This makes this SM-BSM interferrence term insignificant compared to the others. We neglect it in the analysis.

Appendix C

The Matrix Elements of $B^- \to \pi^0 \ell^- \left[\to K^- \nu\right] \bar{\nu}$

In this appendix, elements $\mathcal{M}_{ij}$ of the background process $B^- \to \pi^0 \ell^- \left[\to K^- \nu\right] \bar{\nu}$ are given without further explanation so that they can be used as a reference for future research. These elements are summed to create the full amplitude given in equation 5.17.
The elements $\mathcal{M}_{ij}$ are:

$$\begin{aligned}
\mathcal{M}_{V_{L,L}V_{L,L}} &= \sum_{\ell \text{ spin}} \left[\bar{u}(q_1)\gamma^\alpha P_L u(Q)\right] \left[\bar{u}(Q)\gamma^\mu P_L v(q_2)\right] \langle K^-(k)| \bar{s}\gamma_\alpha P_L u |0\rangle \langle \pi(p')| \bar{u}\gamma_\mu P_L b |B^-(p)\rangle \,, \\
&= \sum_{\ell \text{ spin}} m_\ell \left[\bar{u}(q_1) P_R (\not{Q} + m_\ell) P_R \gamma^\mu v(q_2)\right] \frac{i f_k}{4} \left(f_+(p+p')_\mu + (f_0 - f_+) \frac{M_B^2 - M_\pi^2}{P^2} P_\mu \right) , \\
&= \left[\bar{u}(q_1) P_R \gamma^\mu v(q_2)\right] m_\ell^2 \frac{i f_k}{4} \left(f_+(p+p')_\mu + (f_0 - f_+) \frac{M_B^2 - M_\pi^2}{P^2} P_\mu \right) .
\end{aligned} \tag{C.1}$$

$$\begin{aligned}
\mathcal{M}_{V_{L,L}V_{L,R}} &= \sum_{\ell \text{ spin}} \left[\bar{u}(q_1)\gamma^\alpha P_R u(Q)\right] \left[\bar{u}(Q)\gamma^\mu P_L v(q_2)\right] \langle K^-(k)| \bar{s}\gamma_\alpha P_L u |0\rangle \langle \pi(p')| \bar{u}\gamma_\mu P_L b |B^-(p)\rangle \,, \\
&= \sum_{\ell \text{ spin}} m_\ell \left[\bar{u}(q_1) P_L u(Q)\right] \left[\bar{u}(Q) P_R \gamma^\mu v(q_2)\right] \frac{i f_k}{4} \left(f_+(p+p')_\mu + (f_0 - f_+) \frac{M_B^2 - M_\pi^2}{P^2} P_\mu \right) , \\
&= m_\ell \left[\bar{u}(q_1) P_L \not{Q} \gamma^\mu v(q_2)\right] \frac{i f_k}{4} \left(f_+(p+p')_\mu + (f_0 - f_+) \frac{M_B^2 - M_\pi^2}{P^2} P_\mu \right) .
\end{aligned} \tag{C.2}$$

$$\begin{aligned}
\mathcal{M}_{V_{L,L}S_{L,L}} &= \sum_{\ell \text{ spin}} \left[\bar{u}(q_1) P_R u(Q)\right] \left[\bar{u}(Q)\gamma^\mu P_L v(q_2)\right] \langle K^-(k)| \bar{s} P_L u |0\rangle \langle \pi(p')| \bar{u}\gamma_\mu P_L b |B^-(p)\rangle \,, \\
&= \left[\bar{u}(q_1) P_R (\not{Q} + m_\ell) P_R \gamma^\mu v(q_2)\right] \frac{i f_K M_K^2}{4(m_s + m_u)} \left(f_+(p+p')^\mu + (f_0 - f_+) \frac{M_B^2 - M_\pi^2}{P^2} P^\mu \right) , \\
&= \left[\bar{u}(q_1) P_R \gamma^\mu v(q_2)\right] \frac{i f_K m_\ell M_K^2}{4(m_s + m_u)} \left(f_+(p+p')^\mu + (f_0 - f_+) \frac{M_B^2 - M_\pi^2}{P^2} P^\mu \right) .
\end{aligned} \tag{C.3}$$

$$\begin{aligned}\mathcal{M}_{V_{L,L}S_{L,R}} &= \sum_{\ell\ \text{spin}} [\bar{u}(q_1)P_L u(Q)]\,[\bar{u}(Q)\gamma^\mu P_L v(q_2)]\,\langle K^-(k)|\,\bar{s}P_R u\,|0\rangle\,\langle\pi(p')|\,\bar{u}\gamma_\mu P_L b\,|B^-(p)\rangle\,,\\ &= [\bar{u}(q_1)P_L(\not{Q}+m_\ell)P_R\gamma^\mu v(q_2)]\,\frac{if_K M_K^2}{4(m_s+m_u)}\left(f_+(p+p')^\mu+(f_0-f_+)\frac{M_B^2-M_\pi^2}{P^2}P^\mu\right),\\ &= [\bar{u}(q_1)P_L\not{Q}\gamma^\mu v(q_2)]\,\frac{if_K M_K^2}{4(m_s+m_u)}\left(f_+(p+p')^\mu+(f_0-f_+)\frac{M_B^2-M_\pi^2}{P^2}P^\mu\right).\end{aligned} \tag{C.4}$$

$$\begin{aligned}\mathcal{M}_{V_{L,R}V_{L,L}} &= \sum_{\ell\ \text{spin}} [\bar{u}(q_1)\gamma^\alpha P_L u(Q)]\,[\bar{u}(Q)\gamma^\mu P_R v(q_2)]\,\langle K^-(k)|\,\bar{s}\gamma_\alpha P_L u\,|0\rangle\,\langle\pi(p')|\,\bar{u}\gamma_\mu P_L b\,|B^-(p)\rangle\,,\\ &= m_\ell\,[\bar{u}(q_1)P_R(\not{Q}+m_\ell)P_L\gamma^\mu v(q_2)]\,\frac{if_k}{4}\left(f_+(p+p')_\mu+(f_0-f_+)\frac{M_B^2-M_\pi^2}{P^2}P_\mu\right),\\ &= [\bar{u}(q_1)P_R\not{Q}\gamma^\mu v(q_2)]\,m_\ell^2\frac{if_k}{4}\left(f_+(p+p')_\mu+(f_0-f_+)\frac{M_B^2-M_\pi^2}{P^2}P_\mu\right).\end{aligned} \tag{C.5}$$

$$\begin{aligned}\mathcal{M}_{V_{L,R}V_{L,R}} &= \sum_{\ell\ \text{spin}} [\bar{u}(q_1)\gamma^\alpha P_R u(Q)]\,[\bar{u}(Q)\gamma^\mu P_R v(q_2)]\,\langle K^-(k)|\,\bar{s}\gamma_\alpha P_L u\,|0\rangle\,\langle\pi(p')|\,\bar{u}\gamma_\mu P_L b\,|B^-(p)\rangle\,,\\ &= \sum_{\ell\ \text{spin}} m_\ell\,[\bar{u}(q_1)P_L(\not{Q}+m_\ell)P_L\gamma^\mu v(q_2)]\,\frac{if_k}{4}\left(f_+(p+p')_\mu+(f_0-f_+)\frac{M_B^2-M_\pi^2}{P^2}P_\mu\right),\\ &= [\bar{u}(q_1)P_L\gamma^\mu v(q_2)]\,m_\ell^2\frac{if_k}{4}\left(f_+(p+p')_\mu+(f_0-f_+)\frac{M_B^2-M_\pi^2}{P^2}P_\mu\right).\end{aligned} \tag{C.6}$$

$$\begin{aligned}\mathcal{M}_{V_{L,R}S_{L,L}} &= \sum_{\ell\ \text{spin}} [\bar{u}(q_1)P_R u(Q)]\,[\bar{u}(Q)\gamma^\mu P_R v(q_2)]\,\langle K^-(k)|\,\bar{s}P_R u\,|0\rangle\,\langle\pi(p')|\,\bar{u}\gamma_\mu P_L b\,|B^-(p)\rangle\,,\\ &= [\bar{u}(q_1)P_R(\not{Q}+m_\ell)P_L\gamma^\mu v(q_2)]\,\frac{if_K M_K^2}{4(m_s+m_u)}\left(f_+(p+p')^\mu+(f_0-f_+)\frac{M_B^2-M_\pi^2}{P^2}P^\mu\right),\\ &= [\bar{u}(q_1)P_R\not{Q}\gamma^\mu v(q_2)]\,\frac{if_K M_K^2}{4(m_s+m_u)}\left(f_+(p+p')^\mu+(f_0-f_+)\frac{M_B^2-M_\pi^2}{P^2}P^\mu\right).\end{aligned} \tag{C.7}$$

$$\begin{aligned}\mathcal{M}_{V_{L,R}S_{L,R}} &= \sum_{\ell\ \text{spin}} [\bar{u}(q_1)P_L u(Q)]\,[\bar{u}(Q)\gamma^\mu P_R v(q_2)]\,\langle K^-(k)|\,\bar{s}P_R u\,|0\rangle\,\langle\pi(p')|\,\bar{u}\gamma_\mu P_L b\,|B^-(p)\rangle\,,\\ &= [\bar{u}(q_1)P_L(\not{Q}+m_\ell)P_L\gamma^\mu v(q_2)]\,\frac{if_K M_K^2}{4(m_s+m_u)}\left(f_+(p+p')^\mu+(f_0-f_+)\frac{M_B^2-M_\pi^2}{P^2}P^\mu\right),\\ &= [\bar{u}(q_1)P_L\gamma^\mu v(q_2)]\,\frac{if_K m_\ell M_K^2}{4(m_s+m_u)}\left(f_+(p+p')^\mu+(f_0-f_+)\frac{M_B^2-M_\pi^2}{P^2}P^\mu\right).\end{aligned} \tag{C.8}$$

$$\begin{aligned}\mathcal{M}_{S_{L,L}V_{L,L}} &= \sum_{\ell\ \text{spin}} [\bar{u}(q_1)\gamma^\alpha P_L u(Q)]\,[\bar{u}(Q)P_L v(q_2)]\,\langle K^-(k)|\,\bar{s}\gamma_\alpha P_L u\,|0\rangle\,\langle\pi(p')|\,\bar{u}P_L b\,|B^-(p)\rangle\,,\\ &= \sum_{\ell\ \text{spin}} m_\ell\,[\bar{u}(q_1)P_R(\not{Q}+m_\ell)P_L v(q_2)]\,\frac{if_k f_0}{4}\frac{M_B^2-M_\pi^2}{m_b-m_u},\\ &= [\bar{u}(q_1)P_R\not{Q}\gamma^\mu v(q_2)]\,m_\ell\frac{if_k f_0}{4}\frac{M_B^2-M_\pi^2}{m_b-m_u}.\end{aligned} \tag{C.9}$$

$$\begin{aligned}\mathcal{M}_{S_{L,L}V_{L,R}} &= \sum_{\ell\ \text{spin}} [\bar{u}(q_1)\gamma^\alpha P_R u(Q)]\,[\bar{u}(Q)P_L v(q_2)]\,\langle K^-(k)|\,\bar{s}\gamma_\alpha P_L u\,|0\rangle\,\langle\pi(p')|\,\bar{u}P_L b\,|B^-(p)\rangle\,,\\ &= \sum_{\ell\ \text{spin}} m_\ell\,[\bar{u}(q_1)P_L(\not{Q}+m_\ell)P_L v(q_2)]\,\frac{if_k f_0}{4}\frac{M_B^2-M_\pi^2}{m_b-m_u},\\ &= [\bar{u}(q_1)P_L\gamma^\mu v(q_2)]\,m_\ell^2\frac{if_k f_0}{4}\frac{M_B^2-M_\pi^2}{m_b-m_u}.\end{aligned} \tag{C.10}$$

$$\begin{aligned}\mathcal{M}_{S_{L,L}S_{L,L}} &= \sum_{\ell \text{ spin}} \left[\bar{u}(q_1)P_R u(Q)\right]\left[\bar{u}(Q)P_L v(q_2)\right]\langle K^-(k)|\,\bar{s}P_R u\,|0\rangle\,\langle\pi(p')|\,\bar{u}P_L b\,|B^-(p)\rangle\,,\\ &= \left[\bar{u}(q_1)P_R(\not{Q}+m_\ell)P_L v(q_2)\right]\frac{if_K f_0 M_K^2}{4(m_s+m_u)}\frac{M_B^2-M_\pi^2}{m_b-m_u},\\ &= \left[\bar{u}(q_1)P_R\not{Q}v(q_2)\right]\frac{if_K f_0 M_K^2}{4(m_s+m_u)}\frac{M_B^2-M_\pi^2}{m_b-m_u}.\end{aligned} \tag{C.11}$$

$$\begin{aligned}\mathcal{M}_{S_{L,L}S_{L,R}} &= \sum_{\ell \text{ spin}} \left[\bar{u}(q_1)P_L u(Q)\right]\left[\bar{u}(Q)P_L v(q_2)\right]\langle K^-(k)|\,\bar{s}P_R u\,|0\rangle\,\langle\pi(p')|\,\bar{u}P_L b\,|B^-(p)\rangle\,,\\ &= \left[\bar{u}(q_1)P_L(\not{Q}+m_\ell)P_L v(q_2)\right]\frac{if_K f_0 M_K^2}{4(m_s+m_u)}\frac{M_B^2-M_\pi^2}{m_b-m_u},\\ &= \left[\bar{u}(q_1)P_L v(q_2)\right]m_\ell\frac{if_K f_0 M_K^2}{4(m_s+m_u)}\frac{M_B^2-M_\pi^2}{m_b-m_u}.\end{aligned} \tag{C.12}$$

$$\begin{aligned}\mathcal{M}_{S_{L,R}V_{L,L}} &= \sum_{\ell \text{ spin}} \left[\bar{u}(q_1)\gamma^\alpha P_L u(Q)\right]\left[\bar{u}(Q)P_R v(q_2)\right]\langle K^-(k)|\,\bar{s}\gamma_\alpha P_L u\,|0\rangle\,\langle\pi(p')|\,\bar{u}P_L b\,|B^-(p)\rangle\,,\\ &= m_\ell\left[\bar{u}(q_1)P_R(\not{Q}+m_\ell)P_R v(q_2)\right]\frac{if_0 f_k}{4}\frac{M_B^2-M_\pi^2}{m_b-m_u},\\ &= \left[\bar{u}(q_1)P_R v(q_2)\right]m_\ell^2\frac{if_0 f_k}{4}\frac{M_B^2-M_\pi^2}{m_b-m_u}.\end{aligned} \tag{C.13}$$

$$\begin{aligned}\mathcal{M}_{S_{L,R}V_{L,R}} &= \sum_{\ell \text{ spin}} \left[\bar{u}(q_1)\gamma^\alpha P_R u(Q)\right]\left[\bar{u}(Q)P_R v(q_2)\right]\langle K^-(k)|\,\bar{s}\gamma_\alpha P_L u\,|0\rangle\,\langle\pi(p')|\,\bar{u}P_L b\,|B^-(p)\rangle\,,\\ &= m_\ell\left[\bar{u}(q_1)P_L(\not{Q}+m_\ell)P_R v(q_2)\right]\frac{if_0 f_k}{4}\frac{M_B^2-M_\pi^2}{m_b-m_u},\\ &= \left[\bar{u}(q_1)P_L\not{Q}v(q_2)\right]m_\ell\frac{if_0 f_k}{4}\frac{M_B^2-M_\pi^2}{m_b-m_u}.\end{aligned} \tag{C.14}$$

$$\begin{aligned}\mathcal{M}_{S_{L,R}S_{L,L}} &= \sum_{\ell \text{ spin}} \left[\bar{u}(q_1)P_R u(Q)\right]\left[\bar{u}(Q)P_R v(q_2)\right]\langle K^-(k)|\,\bar{s}P_R u\,|0\rangle\,\langle\pi(p')|\,\bar{u}P_L b\,|B^-(p)\rangle\,,\\ &= \left[\bar{u}(q_1)P_R(\not{Q}+m_\ell)P_R v(q_2)\right]\frac{if_K f_0 M_K^2}{4(m_s+m_u)}\frac{M_B^2-M_\pi^2}{m_b-m_u},\\ &= \left[\bar{u}(q_1)P_R v(q_2)\right]m_\ell\frac{if_K f_0 M_K^2}{4(m_s+m_u)}\frac{M_B^2-M_\pi^2}{m_b-m_u}.\end{aligned} \tag{C.15}$$

$$\begin{aligned}\mathcal{M}_{S_{L,R}S_{L,R}} &= \sum_{\ell \text{ spin}} \left[\bar{u}(q_1)P_L u(Q)\right]\left[\bar{u}(Q)P_R v(q_2)\right]\langle K^-(k)|\,\bar{s}P_R u\,|0\rangle\,\langle\pi(p')|\,\bar{u}P_L b\,|B^-(p)\rangle\,,\\ &= \left[\bar{u}(q_1)P_L(\not{Q}+m_\ell)P_R v(q_2)\right]\frac{if_K f_0 M_K^2}{4(m_s+m_u)}\frac{M_B^2-M_\pi^2}{m_b-m_u},\\ &= \left[\bar{u}(q_1)P_L\not{Q}v(q_2)\right]\frac{if_K f_0 M_K^2}{4(m_s+m_u)}\frac{M_B^2-M_\pi^2}{m_b-m_u}.\end{aligned} \tag{C.16}$$

$$\begin{aligned}\mathcal{M}_{T_L V_{L,L}} &= \sum_{\ell \text{ spin}} \left[\bar{u}(q_1)\gamma^\alpha P_L u(Q)\right]\left[\bar{u}(Q)\sigma^{\mu\nu}P_L v(q_2)\right]\langle K^-(k)|\,\bar{s}\gamma_\alpha P_L u\,|0\rangle\,\langle\pi(p')|\,\bar{u}\sigma_{\mu\nu}b\,|B^-(p)\rangle\,,\\ &= \left[\bar{u}(q_1)P_R(\not{Q}+m_\ell)P_L\sigma^{\mu\nu}v(q_2)\right]\frac{-m_\ell f_K f_T}{4(M_B+M_\pi)}\left[P_\nu(p+p')_\mu-(p+p')_\nu P_\mu\right],\\ &= \left[\bar{u}(q_1)P_R\not{Q}\sigma^{\mu\nu}v(q_2)\right]\frac{-m_\ell f_K f_T}{4(M_B+M_\pi)}\left[P_\nu(p+p')_\mu-(p+p')_\nu P_\mu\right].\end{aligned} \tag{C.17}$$

$$\mathcal{M}_{T_L V_{L,R}} = \sum_{\ell \text{ spin}} [\bar{u}(q_1)\gamma^\alpha P_R u(Q)]\,[\bar{u}(Q)\sigma^{\mu\nu} P_L v(q_2)]\,\langle K^-(k)|\,\bar{s}\gamma_\alpha P_L u\,|0\rangle\,\langle \pi(p')|\,\bar{u}\sigma_{\mu\nu} b\,|B^-(p)\rangle\,,$$

$$= [\bar{u}(q_1)P_L(\not{Q} + m_\ell)P_L\sigma^{\mu\nu}v(q_2)]\,\frac{-m_\ell f_K f_T}{4(M_B+M_\pi)}\,[P_\nu(p+p')_\mu - (p+p')_\nu P_\mu]\,, \tag{C.18}$$

$$= [\bar{u}(q_1)P_L\sigma^{\mu\nu}v(q_2)]\,\frac{-m_\ell^2 f_K f_T}{4(M_B+M_\pi)}\,[P_\nu(p+p')_\mu - (p+p')_\nu P_\mu]\,.$$

$$\mathcal{M}_{T_L S_{L,L}} = \sum_{\ell \text{ spin}} [\bar{u}(q_1)P_R u(Q)]\,[\bar{u}(Q)\sigma^{\mu\nu} P_L v(q_2)]\,\langle K^-(k)|\,\bar{s}P_R u\,|0\rangle\,\langle \pi(p')|\,\bar{u}\sigma_{\mu\nu} b\,|B^-(p)\rangle\,,$$

$$= [\bar{u}(q_1)P_R(\not{Q} + m_\ell)P_L\sigma^{\mu\nu}v(q_2)]\,\frac{-f_K f_T M_K^2}{4(M_B+M_\pi)(m_s+m_u)}\,[P_\nu(p+p')_\mu - (p+p')_\nu P_\mu]\,, \tag{C.19}$$

$$= [\bar{u}(q_1)P_R\not{Q}\sigma^{\mu\nu}v(q_2)]\,\frac{-f_K f_T M_K^2}{4(M_B+M_\pi)(m_s+m_u)}\,[P_\nu(p+p')_\mu - (p+p')_\nu P_\mu]\,.$$

$$\mathcal{M}_{T_L S_{L,R}} = \sum_{\ell \text{ spin}} [\bar{u}(q_1)P_L u(Q)]\,[\bar{u}(Q)\sigma^{\mu\nu} P_L v(q_2)]\,\langle K^-(k)|\,\bar{s}P_R u\,|0\rangle\,\langle \pi(p')|\,\bar{u}\sigma_{\mu\nu} b\,|B^-(p)\rangle\,,$$

$$= [\bar{u}(q_1)P_L(\not{Q} + m_\ell)P_L\sigma^{\mu\nu}v(q_2)]\,\frac{-f_K f_T M_K^2}{4(M_B+M_\pi)(m_s+m_u)}\,[P_\nu(p+p')_\mu - (p+p')_\nu P_\mu]\,, \tag{C.20}$$

$$= [\bar{u}(q_1)P_L\sigma^{\mu\nu}v(q_2)]\,\frac{-f_K f_T m_\ell M_K^2}{4(M_B+M_\pi)(m_s+m_u)}\,[P_\nu(p+p')_\mu - (p+p')_\nu P_\mu]\,.$$

$$\mathcal{M}_{T_R V_{L,L}} = \sum_{\ell \text{ spin}} [\bar{u}(q_1)\gamma^\alpha P_L u(Q)]\,[\bar{u}(Q)\sigma^{\mu\nu} P_R v(q_2)]\,\langle K^-(k)|\,\bar{s}\gamma_\alpha P_L u\,|0\rangle\,\langle \pi(p')|\,\bar{u}\sigma_{\mu\nu} b\,|B^-(p)\rangle\,,$$

$$= [\bar{u}(q_1)P_R(\not{Q} + m_\ell)P_R\sigma^{\mu\nu}v(q_2)]\,\frac{-m_\ell f_K f_T}{4(M_B+M_\pi)}\,[P_\nu(p+p')_\mu - (p+p')_\nu P_\mu]\,, \tag{C.21}$$

$$= [\bar{u}(q_1)P_R\sigma^{\mu\nu}v(q_2)]\,\frac{-m_\ell^2 f_K f_T}{4(M_B+M_\pi)}\,[P_\nu(p+p')_\mu - (p+p')_\nu P_\mu]\,.$$

$$\mathcal{M}_{T_R V_{L,R}} = \sum_{\ell \text{ spin}} [\bar{u}(q_1)\gamma^\alpha P_R u(Q)]\,[\bar{u}(Q)\sigma^{\mu\nu} P_R v(q_2)]\,\langle K^-(k)|\,\bar{s}\gamma_\alpha P_L u\,|0\rangle\,\langle \pi(p')|\,\bar{u}\sigma_{\mu\nu} b\,|B^-(p)\rangle\,,$$

$$= [\bar{u}(q_1)P_L(\not{Q} + m_\ell)P_R\sigma^{\mu\nu}v(q_2)]\,\frac{-m_\ell f_K f_T}{4(M_B+M_\pi)}\,[P_\nu(p+p')_\mu - (p+p')_\nu P_\mu]\,, \tag{C.22}$$

$$= [\bar{u}(q_1)P_L\not{Q}\sigma^{\mu\nu}v(q_2)]\,\frac{-m_\ell f_K f_T}{4(M_B+M_\pi)}\,[P_\nu(p+p')_\mu - (p+p')_\nu P_\mu]\,.$$

$$\mathcal{M}_{T_R S_{L,L}} = \sum_{\ell \text{ spin}} [\bar{u}(q_1)P_R u(Q)]\,[\bar{u}(Q)\sigma^{\mu\nu} P_R v(q_2)]\,\langle K^-(k)|\,\bar{s}P_R u\,|0\rangle\,\langle \pi(p')|\,\bar{u}\sigma_{\mu\nu} b\,|B^-(p)\rangle\,,$$

$$= [\bar{u}(q_1)P_R(\not{Q} + m_\ell)P_R\sigma^{\mu\nu}v(q_2)]\,\frac{-f_K f_T M_K^2}{4(M_B+M_\pi)(m_s+m_u)}\,[P_\nu(p+p')_\mu - (p+p')_\nu P_\mu]\,, \tag{C.23}$$

$$= [\bar{u}(q_1)P_R\sigma^{\mu\nu}v(q_2)]\,\frac{-f_K f_T M_K^2 m_\ell}{4(M_B+M_\pi)(m_s+m_u)}\,[P_\nu(p+p')_\mu - (p+p')_\nu P_\mu]\,.$$

$$\mathcal{M}_{T_R S_{L,R}} = \sum_{\ell \text{ spin}} [\bar{u}(q_1)P_L u(Q)]\,[\bar{u}(Q)\sigma^{\mu\nu} P_R v(q_2)]\,\langle K^-(k)|\,\bar{s}P_R u\,|0\rangle\,\langle \pi(p')|\,\bar{u}\sigma_{\mu\nu} b\,|B^-(p)\rangle\,,$$

$$= [\bar{u}(q_1)P_L(\not{Q} + m_\ell)P_R\sigma^{\mu\nu}v(q_2)]\,\frac{-f_K f_T M_K^2}{4(M_B+M_\pi)(m_s+m_u)}\,[P_\nu(p+p')_\mu - (p+p')_\nu P_\mu]\,, \tag{C.24}$$

$$= [\bar{u}(q_1)P_L\not{Q}\sigma^{\mu\nu}v(q_2)]\,\frac{-f_K f_T M_K^2}{4(M_B+M_\pi)(m_s+m_u)}\,[P_\nu(p+p')_\mu - (p+p')_\nu P_\mu]\,.$$